Agilent
MIMO Channel Modeling and Emulation Test Challenges

Application Note

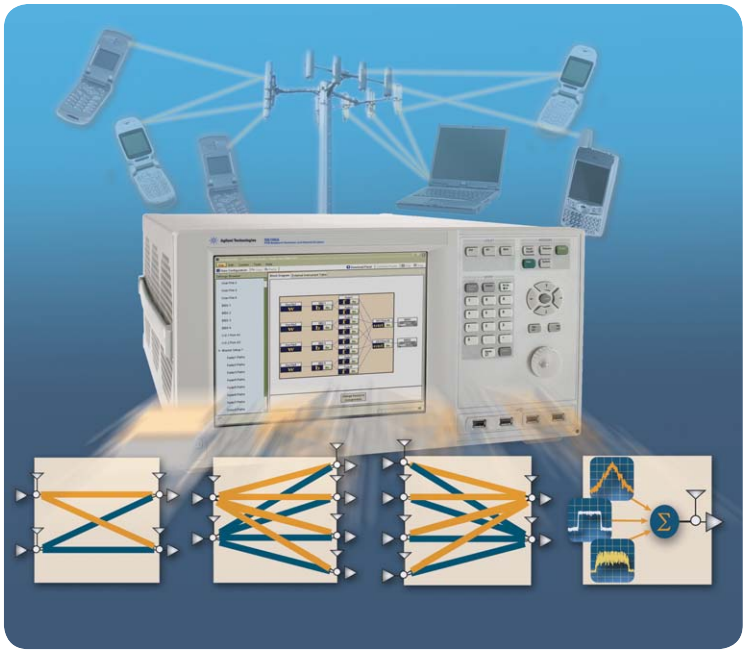

This application note begins with a review of MIMO technologies and the basic properties of wireless channels and goes on to introduce the concepts of spatial correlation and its effects on MIMO performance. It also includes a demonstration of modeling the spatial characteristics of MIMO channels and describes how these complex channels can be emulated using commercially available instrumentation such as the Agilent N5106A PXB baseband generator and signal emulator.

Agilent Technologies

Table of Contents

Introduction

Multiple Input Multiple Output (MIMO) technology holds the promise of higher data rates with increased spectral efficiency. Due to the potential improvement in system performance and advances in digital signal processing, many wireless systems, including the IEEE 802.11n wireless LAN, IEEE 802.16e-based Mobile WiMAX™ Wave 2 and the Long-Term Evolution (LTE) mobile wireless system, have recently adopted the use of MIMO and multiple antenna technologies. All of these commercial wireless systems operate in high multipath environments and it is the benefit of multipath that provides the performance improvement when using multiple antenna configurations.

While MIMO offers the potential for increased signal robustness and capacity improvement when operating in rich multipath environments, developing and testing MIMO components and systems requires advanced channel emulation tools that are easily configured and provide an accurate representation of realistic wireless channels and conditions.

This application note begins with a review of MIMO technologies and the basic properties of wireless channels and goes on to introduce the concepts of spatial correlation and its effects on MIMO performance. It also includes a demonstration of modeling the spatial characteristics of MIMO channels and describes how these complex channels can be emulated using commercially available instrumentation such as the Agilent N5106A PXB baseband generator and signal emulator which will be referred to throughout the remainder of this document as the PXB.

Reviewing MIMO Technologies

Multiple antennas placed at the transmitter and/or receiver in wireless communication systems can be used to substantially improve system performance by leveraging the "spatial" characteristics of the wireless channel. These systems, now widely termed as Multiple Input Multiple Output (MIMO), require two or more antennas placed at the transmitter and at the receiver. In MIMO terminology, the "Input" and "Output" are referenced to the wireless channel. In these systems, performance gains are achieved as multiple transmitters simultaneously **input** their signal into the wireless channel and then combinations of these signals simultaneously **output** from the wireless channel into the multiple receivers. In a practical system for the downlink communication, a single Basestation (BS) would contain multiple transmitters connected to multiple antennas and a single Mobile Station (MS) would contain multiple antennas connected to multiple receivers. This same configuration may be used in the uplink. Figure 1 shows several basic block diagrams for connecting each transmitter to each receiver in a wireless system using multiple antennas. Each arrow represents the combination of all signal paths between two antennas that include the direct Line of Sight (LOS) path, should one exist, and the numerous multipath signals created from reflection, scattering and diffraction from the surrounding environment. For example, Single Input Single Output (SISO) is the traditional configuration for radio and television broadcast and early 1st generation cellular. This single channel includes the LOS path and all multipaths present over the wireless link. The Single Input Multiple Output (SIMO) and Multiple Input Single Output (MISO) configurations require the use of a single antenna at either the transmitter or the receiver. The SIMO case may be useful when transmitting uplink data from a mobile device, which has a single antenna, to a cellular base station or WLAN access point containing two or more antennas. Alternately, the MISO case may represent the configuration for the downlink transmission of data with transmit diversity. Figure 1 also shows a 2x2 MIMO configuration where two antennas are placed at the transmitter which has two separate transmit channels and two antennas at the receiver which has two separate receive channels. This configuration will be discussed as the primary example in this application note. There are obviously numerous other MIMO configurations using other combinations of multiple antenna pairs, such as 3x3 and 4x4. MIMO operation does not require an equal number of antennas at the transmitter and receiver as there may be more antennas at one location than another, such as an M x N configuration where M does not equal N and M equals the number of transmit antennas and N equals the number of receive antennas.

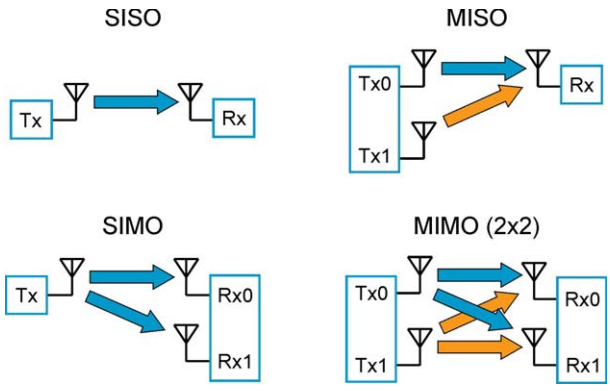

Figure 1. Antenna and channel configurations for SISO, SIMO, MISO and MIMO (2x2) systems.

Multiple antenna techniques

Multiple antenna systems take advantage of the spatial diversity obtained by placing separate antennas in a dense multipath scattering environment. These systems may be implemented in a number of different ways to obtain either a diversity gain to combat signal fading or to obtain a capacity improvement. Generally, there are three categories of multiple antenna techniques. The first one aims to improve the power efficiency by maximizing **spatial diversity**. Such techniques include delay diversity, space-time block codes (STBC), and space-time trellis codes (STTC). The second type uses **spatial multiplexing**, defined as MIMO, where under rich scattering environments, independent data streams are simultaneously transmitted over different antennas to increase the effective data rate. The third type of multiple antenna system exploits knowledge of the channel at the transmitter, also termed as **beamforming**. It utilizes the channel information to build the beamforming matrices as pre- and post-filters at the transmitter and receiver to achieve capacity gain.

Spatial diversity

Signal power in a wireless channel fluctuates rapidly over time and distance due to the rich multipath environment. When the signal power drops significantly at the receiver, the channel is said to be in a multipath fade. Diversity is often used in wireless channels to combat this fading effect. Antenna diversity combats fading by combining signals from two or more independently faded channels. For example, in a SIMO system, receive antenna diversity will improve system performance when the receiver optimally combines signals from separate antennas so that the resultant signal exhibits a reduced amplitude variation when compared to the signal amplitude from any one antenna. Diversity is characterized by the number of independently fading channels, also known as diversity order, and is equal to the number of receive antennas in a SIMO configured system. It is important to note that if the fading channels are not independent, or in other words correlated, then antenna diversity may not improve the system performance.

Transmit diversity is applicable to MISO channels and has become an active area of research. If the channels from each transmit antenna to the single receive antenna have independent fading characteristics, then the diversity order is equal to the number of transmit antennas. If the transmitter does not have prior knowledge of the channel characteristics then a suitable design of the transmitted signal is required to achieve diversity gain at the receiver. One very popular transmit diversity technique that has recently gained much attention is Space Time Coding (STC). This technique sends the same user data to both transmit antennas, but at different times, for improving the probability of successfully recovering the desired data. The STC process effectively encodes the data in both space and time.

A simplified block diagram using Alamouti STC is shown in Figure 2. In this system, two different symbols are simultaneously transmitted from the two antennas during any symbol period. During the first time period, the first symbol in the sequence, s0, is transmitted from the upper antenna #1 while the second symbol, s1, is simultaneously transmitted from the lower antenna #2. During the next symbol time the signal -s1* is transmitted from the upper antenna and the signal s0* is transmitted from lower antenna. Note that ( )* is the complex conjugate operation. Keep in mind that the data symbols are complex numbers relating to the selected modulation scheme, for example, when using QPSK modulation, the data symbols are representative of the four constellation points in the IQ vector diagram. At the receiver, a single antenna receives a combination of the two transmitted signals after transmission through the multipath environment. The channel coefficient, h0, represents the magnitude and phase of the transmission path between transmit antenna #1 and the receive antenna. The channel coefficient, h1, represents the path between transmit antenna #2 and the receive antenna. Note that the channel coefficients, h0 and h1, are complex numbers that represent the total amplitude and phase of their respective channels including all multipath effects.

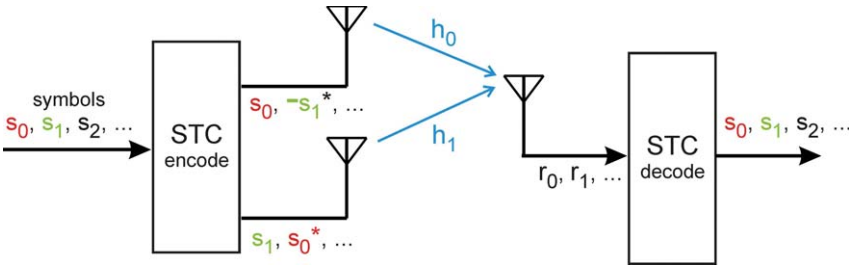

Figure 2. Simplified Alamouti Space Time Coding (STC) block diagram.

During the first symbol time shown in Figure 2, the received signal, r0, is the combination of both symbols, s0 and s1, but is modified by the channel coefficients, h0 and h1. During the next symbol period, the receiver measures r1 which contain modified versions of s0 and s1. The received signals, r0 and r1, as a function of the transmitted signals and channels coefficients can be represented as

$$r_0 = h_0 s_0 + h_1 + s_1 \qquad \textit{Equation 1}$$

$$r_1 = h_1 s_0^* + h_0 (- s_1^*) \qquad \textit{Equation 2}$$

In order to recover the actual transmitted symbols, s0 and s1, the receiver requires knowledge of the channel coefficients, h0 and h1. These channel coefficients are often estimated at the receiver by measuring known signals embedded in the transmitted waveforms. For example, in a WiMAX Wave 2 signal, the OFDM waveform is designed such that pilot subcarriers transmitted on one transmitter channel do not overlap in time with pilot subcarriers on the other transmitter channel. If the pilot waveforms are known at the receiver, then the channel coefficients can be estimated from the associated receiver measurements. Once the channel coefficients are accurately known by the receiver, Equations 1 and 2 can be rearranged in terms of the desired data, s0 and s1. In this case the receiver can properly decode the desired symbols using the received signals, r0 and r1, measured over two consecutive symbol times using the following equations.

$$s_0 = A(h_0^* r_0 + h_1 r_0^*) \qquad \textit{Equation 3}$$

$$s_1 = A(h_1^* s_0 - h_0 r_1^*) \qquad \textit{Equation 4}$$

$$\text{where } A = \frac{1}{|h_0|^2 + |h_1|^2} \qquad \textit{Equation 5}$$

It should be noted that this diversity technique does not improve the system data rate but rather improves the signal quality. The sequence shown in Figure 2 uses encoding performed in space and time (space–time coding). The encoding may also be done over the space and frequency domains. In this case, instead of two consecutive symbol periods transmitted from two separate antennas, two frequency carriers may be used (space–frequency coding).

Utilization of diversity in MIMO channels requires a combination of the transmit and receive diversity described above. The diversity order would then be equal to the product of the number of transmit and receive antennas if the channel between each transmit-receive antenna pair fades independently.

Spatial Multiplexing

Spatial multiplexing can offer an increase in the transmission rate, while using the same bandwidth and power as in a traditional SISO system. The theoretical increase in capacity is linearly related to the number of transmit/receive antenna pairs added to the MIMO system. A MIMO system can also be configured with an unequal number of antennas at the transmitter and the receiver, such as an MxN case where M transmit antennas does not equal N receive antennas. In this configuration, the capacity improvement is proportional to the smaller number, M or N.

Figure 3 shows a simple spatial multiplexing system using a 2x2 MIMO configuration. This concept can easily be extended to more general MxN MIMO systems. In this example, the first data symbol, s0, is transmitted from the upper transmit antenna, Tx0, and the second data symbol, s1, is transmitted from lower antenna transmit antenna, Tx1. The transmission of these two data symbols occurs simultaneously during the first symbol time. During the next symbol time, data symbols s2 and s3 are simultaneously transmitted. In this process, the data rate is doubled as alternate symbols are transmitted from each antenna and each symbol is only transmitted once. This technique is different from STC where data symbols are repeated over two symbol times across the two antennas.

Transmission of the signal from transmit antenna Tx0 to the receive antenna Rx0 occurs over the wireless channels with a complex channel coefficient *h00*. Transmission from antenna Tx0 to the antenna Rx1 occurs over the wireless channel with a complex channel coefficient *h10*. By properly placing the antennas it can be assumed that these two channel coefficients are different. There is a similar relationship between Tx1 and the two receive antennas resulting in a total of four potentially unique channel coefficients, *h00, h10, h01* and *h11*.

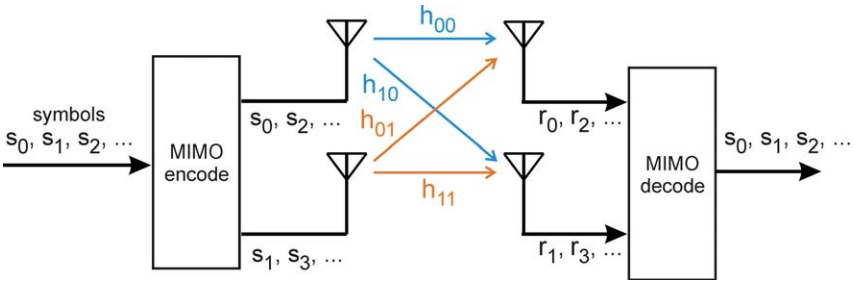

Figure 3. Simplified 2x2 MIMO block diagram.

After transmission through the channel, the receiver measures the signal, r0, at the upper antenna, Rx0, as a combination of the s0 and s1 including channel effects, *h00* and *h01*. At the same time, the lower antenna measures r1 as a combination of s0 and s1 modified by the channel effects, *h10* and *h11* respectively. The equations for r0 and r1 as a function of transmitted symbols and channel coefficients can be represented as

$$r_0 = h_{00}s_0 + h_{01}s_1 \qquad \textit{Equation 6}$$

$$r_1 = h_{10}s_0 + h_{11}s_1 \qquad \textit{Equation 7}$$

Under favorable channel conditions, the spatial signatures of the two signals, r0 and r1, are well separated. The receiver, having knowledge of the channel coefficients, can differentiate and recover symbols, s0 and s1. The equations for calculating s0 and s1 based on measurements of r0 and r1 and the channel coefficients are

$$s_0 = B(h_{11}r_0 - h_{01}r_1) \qquad \textit{Equation 8}$$

$$s_1 = B(-h_{10}r_0 + h_{00}r_1) \qquad \textit{Equation 9}$$

$$\text{where } B = \frac{1}{h_{00}h_{11} - h_{01}h_{10}} \qquad \textit{Equation 10}$$

After decoding, the sub-streams are multiplexed into the original symbol stream. Spatial multiplexing increases transmission rates proportionally with the number of transmit-receive antenna pairs.

Spatial multiplexing also can be applied in a multiuser format, also known as Space Division Multiple Access (SDMA). Consider two mobile users transmitting their individual signals over the same wireless channel that arrive at a base-station equipped with two antennas. The base-station can separate the two signals using the spatial multiplexing technique described above. The increase in capacity is proportional to the number of antennas at the base-station or the number of mobile users, whichever number is smaller. This technique has been defined in the WiMAX Wave 2 standard and is termed Uplink Collaborative Spatial Multiplexing (UL-CSM).

It is important to note that spatial multiplexing can only increase transmission rates when the wireless environment is very rich in multipath. The rich multipath will result in low correlations between the channels, making data recovery possible at the receiver. When the channels are highly correlated, the spatial multiplexing performance rapidly degrades. In mathematical terms, Equations 6 and 7 above can be written in matrix form as

$$\begin{bmatrix} r_0 \\ r_1 \end{bmatrix} = \begin{bmatrix} h_{00} & h_{01} \\ h_{10} & h_{11} \end{bmatrix} \begin{bmatrix} s_0 \\ s_1 \end{bmatrix} \qquad \textit{Equation 11}$$

$$[R] = [H][S] \qquad \textit{Equation 12}$$

In order to correctly recover the data symbols at the receiver, Equation 12 is rearranged in matrix form as

$$[S] = [H]^{-1}[R] \qquad \textit{Equation 13}$$

The channel coefficient matrix [H] needs to be inverted in order to retrieve the data from the received signals. If the channel coefficients in [H] are highly correlated, matrix inversion becomes difficult and the matrix is considered "ill-conditioned". In this technique, an ill-conditioned [H] matrix causes the calculation of s0 and s1 to become very sensitive to small changes in the values of the calculated channel coefficients and measured values of r0 and r1. Therefore, any noise in the system may greatly affect the recovery of s0 and s1.

Beamforming

In a traditional beamforming application, the same signal, or data symbol, is simultaneously transmitted from each antenna element after a complex weight (magnitude and/or phase) is applied to each signal path in order to "steer" the antenna array for optimal SNR over the wireless link. In a beamformer optimized for spatial diversity or spatial multiplexing, each antenna element simultaneously transmits a weighted combination of two data symbols. This beamforming technique requires knowledge of the channel characteristics at the transmitter, which was not a requirement for the spatial diversity and spatial multiplexing techniques previously discussed. In this case, it may be required to measure the channel at the receiver and send information back to the transmitter. The channel knowledge at the transmitter can be full or partial. Full channel knowledge implies that the channel matrix [H] is known to the transmitter. Partial knowledge might refer to some parameters of the instantaneous channel, such as the channel matrix's condition number or a statistical property related to the transmit and/or receive correlation characteristics. The condition number is the ratio of the largest singular value over the smallest singular value. It provides an indication of the accuracy in the matrix inversion, which determines the suitability for MIMO multiplexing. A condition number near 1 (0 dB) indicates a well-conditioned matrix whereas a value larger than 6 dB indicates a poorly defined channel matrix. Signal analyzers such as the Agilent 89600-series Vector Signal Analyzer can directly measure the MIMO condition number.

A pre-coding framework for exploiting channel knowledge at the transmitter is shown in Figure 4. The symbols to be transmitted, s_0, s_1, s_2, s_3, ..., are multiplied by a weighting function that can be interpreted as the beamformer. After applying the pre-coding weights, two separate data streams are simultaneously transmitted from two transmit antennas as spatial multiplexing. As shown in Figure 4, during the first symbol time, the data, x0, transmitted from the upper antenna is a linear combination of the first two data symbols, s0 and s1. During this same time, the lower antenna transmits data x1 that represents a different combination of these two symbols, thus effectively doubling the data rate. Here, the transmitted data is related to the input symbols by the following equations.

$$x_0 = w_{00}s_{00} + w_1s_1 \qquad \textit{Equation 14}$$

$$x_1 = w_{10}s_0 + w_{11}s_1 \qquad \textit{Equation 15}$$

Denote the 2x2 pre-coding matrix as [*W*], and then in matrix form, the transmitted signals are related by

$$\begin{bmatrix} x_0 \\ x_1 \end{bmatrix} = \begin{bmatrix} w_{00} & w_{01} \\ w_{10} & w_{11} \end{bmatrix} \begin{bmatrix} s_0 \\ s_1 \end{bmatrix} \qquad \textit{Equation 16}$$

$$[X] = [W][S] \qquad \textit{Equation 17}$$

For this pre-coding scheme, the transmission rate also increases proportionally with the number of transmit-receive antenna pairs, as was the case for spatial multiplexing discussed above, but the additional flexibility for optimizing the signal transmission into the wireless channel at the transmitter may also improve the relative system performance.

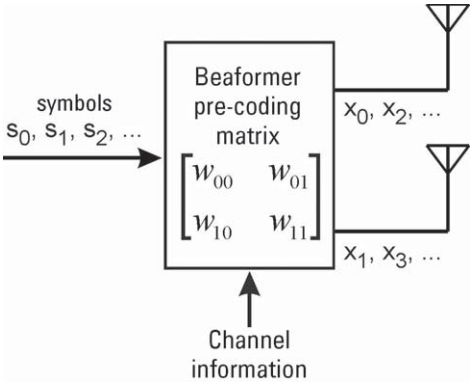

Figure 4. Beamforming transmit encoder.

MIMO in wireless standards

MIMO technologies hold the promise of higher data rates with increased spectral efficiency. Due to the large potential improvement in wireless system performance, many standards committees have recently adopted or are considering the use of MIMO and multiple antenna technologies. For instance, the International Telecommunications Union (ITU) working group has integrated MIMO techniques into the high-speed downlink packet access (HSDPA) channel,[1, 2] which is a part of the Universal Mobile Telecommunications System (UMTS) standard. In WLAN systems, MIMO applications have been defined in the IEEE 802.11n standard.[3, 4] In mobile broadband wireless access (BWA), MIMO has also been adopted into the IEEE 802.16 standard that is the basis for Mobile WiMAX,[5, 6] which is the standard on which Mobile WiMAX[7,8] Wave 2 profiles are based. Lastly, the evolving LTE standard[9, 10] has included MIMO into the current roadmap. All of these commercial wireless systems operate in high multipath environments and it is the benefit of rich multipath characteristics that provides the performance improvement when using multiple antenna systems.

1. Agilent Application Note, *Concepts of High Speed Downlink Packet Access: Bringing Increased Throughput and Efficiency to W-CDMA*, Literature number 5989-2365EN, January 18, 2007.
2. Additional information about HSDPA can be found at **http://www.agilent.com/find/HSDPA**.
3. Agilent Application Note 1509, *MIMO Wireless LAN PHY Layer [RF] Operation & Measurement*, Literature number 5989-3443EN, September 16, 2005.
4. Additional information about 802.11n WLAN can be found at **http://www.agilent.com/find/WLAN**.
5. Additional information about the IEEE 802.16 specification and working group can be found at **http://www.ieee802.org/16/**.
6. Agilent Application Note 1578, *IEEE 802.16e WiMAX OFDMA Signal Measurements and Troubleshooting*, Literature number 5989-2382EN, June 6, 2006.
7. For more information about WiMAX, visit **http://www.wimaxforum.org**.
8. For more information about test solutions for WiMAX, visit **http://www.agilent.com/find/wimax**.
9. For more information about the 3GPP and LTE specifications visit the 3GPP home page at **http://www.3gpp.org/**.
10. For more information about Agilent design and test products for LTE visit **http://www.agilent.com/find/LTE**.

Channel correlation effects on MIMO performance

For wireless communication systems, the wireless channel is the key factor that determines system performance. Channel effects, such as path loss and multipath fading, result in the attenuation of the signal amplitude at the receiver. Multipath may also induce inter-symbol interference if the delay spread is longer than the cyclic prefix in an OFDM signal. Spatial diversity and spatial multiplexing have been shown, both theoretically and experimentally, to substantially improve performance and overcome the undesired effects of multipath but only if the spatial dimension is properly configured to leverage the richness of the multipath environment.

As introduced above, the diversity gain achievable using STC is dependent on the channel diversity order. Only when the channels between each transmit-receive antenna pair fade independently will the channel diversity order be equal to the product of the number of transmit and receive antennas. Alternately, if the channels between transmit-receive antenna pairs are highly correlated, then the achievable diversity gain is very limited.

Low correlation channels are also required in spatial multiplexing MIMO applications. The different spatial signal streams can be well separated only under favorable channel conditions. This often requires proper positioning of the transmit and receive antennas in order to provide low channel-to-channel correlations between the antenna pairs.

As a measurement example, Figure 5 shows the 2x2 MIMO channel coefficients, h_{00}, h_{10}, h_{01}, and h_{11}, for two different fading channels, one with relatively high channel-to-channel correlations and the other with low correlations. These measurements were made using an Agilent dual-channel 89600-series vector signal analyzer (VSA) on a WiMAX OFDMA signal that was faded using the PXB. The plot on the upper left shows the four channel coefficients as a function of subcarrier frequency for the high correlation case. It can be observed that the magnitude of the coefficients have a similar frequency response resulting from the high degree of correlation between some of the paths. The lower plot displays the measured constellation for the demodulated symbols which shows a high level of signal corruption. As a comparison, the figure on the upper right shows the coefficients for low channel-to-channel correlations. In this case, the frequency responses of the coefficients are dissimilar, resulting in an improvement in the MIMO symbol recovery, as shown by the measured constellation in the lower right of Figure 5.

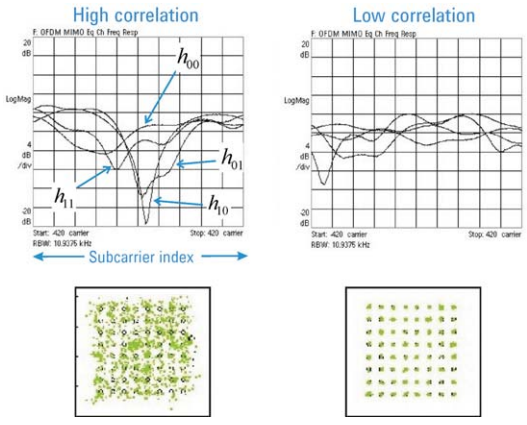

Figure 5. Measured channel coefficients and demodulated constellations for a 2x2 MIMO waveform.

Challenges in emulating MIMO channels

Testing MIMO receivers and systems under realistic channel environments can often be challenging due to the large number of transmit-receive channel combinations. For example, in a 2x2 MIMO configuration, using two separate SISO channel emulators is not adequate to model the four separate channels that exist between the pairs of transmit and receive antennas. In addition, SISO channel emulators do not provide any correlation between channels, which was previously shown to be an important characteristic when testing system performance. Testing directly in a "real" wireless environment is not an effective method, especially during the design and validation stages, as the channel is very sensitive, not controllable, and not repeatable. Also, testing in a real channel is not practical when different environments are required and when mobility testing is also necessary.

Creating realistic MIMO channels using software tools is another option but is often time-consuming and produces results that are not real-time. For example, after creating the channel fading coefficients in software, the convolution of these coefficients with the transmitted signals is a relatively long process preventing real-time performance. In some types of software-based test systems, the modulated data and faded signals are used to create complex (I/Q) waveforms that are downloaded into the memory of an arbitrary waveform generator (ARB) for playback. The ARBs may be internal to the RF signal generator, such as those in the Agilent E4438C ESG signal generators, or external to the RF signal generator, such as the Agilent N6030A-series arbitrary waveform generators. There are many software tools that can accelerate the creation of faded waveforms, such as Agilent Signal Studio, Mathworks MATLAB™ and Agilent Advanced Design System (ADS), but these tools are often limited to traditional fading models. In addition, the arbitrary waveform generators have limited playback memory resulting in relatively short waveforms that repeat over time. Therefore, specialized instrumentation that emulates realistic MIMO channels provides the best solution for these challenging test conditions.

A channel emulator, such as the PXB, that replicates real-world MIMO conditions using powerful digital signal processing technology will make it possible to rapidly isolate performance issues early in the design, development and verification cycle, and provide the quickest path for troubleshooting advanced radio components and systems. The channel emulator also has the advantages that it can generate realistic fading scenarios including path and channel correlations, and has a lower implementation cost and a faster calibration process. The PXB provides up to 4 baseband generators and 8 faders useful for testing and troubleshooting up to 4x2 MIMO systems. Figure 6 shows a simplified configuration diagram for testing a 2x2 MIMO receiver using the PXB connected with two RF signal generators for signal upconversion. The PXB internal baseband generators create the standards-compliant waveforms such as WiMAX, LTE and WLAN signals. These baseband generators are easily connected to the channel faders through a software GUI. Each fader can be independently configured with a standards-compliant fading model, such as a WiMAX ITU Pedestrian B, or custom configured model using a variety of path and fading conditions.

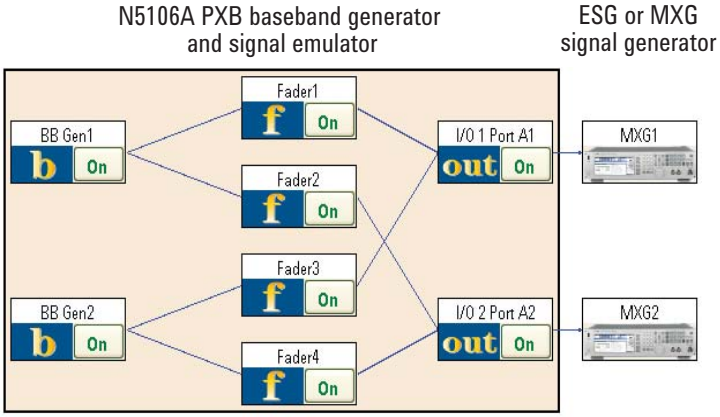

Figure 6. Simplified block diagram for testing a 2x2 MIMO receiver using the PXB.

MIMO Channel Overview

A signal propagating through a wireless channel arrives at the destination along a number of different paths, referred to as multipath. Figure 7 is a diagram of a typical mobile subscriber driving along a roadway. It depicts three of the many signal paths from the transmitter to receiver. These paths arise from scattering, reflection and diffraction of the radiated energy by objects in the environment or refraction in the medium. The various propagation mechanisms influence path loss and fading models differently.

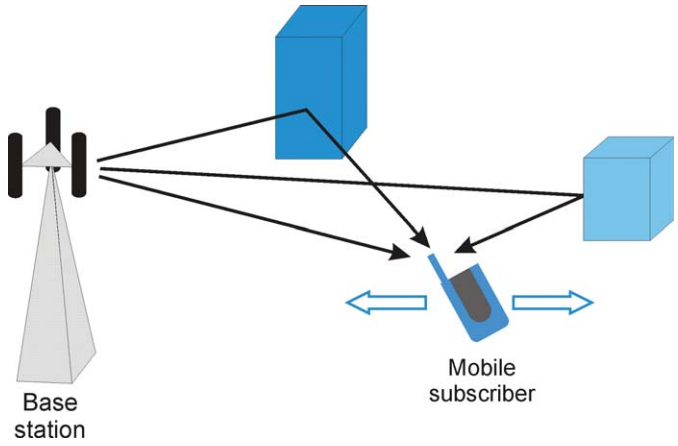

Figure 7. Typical multipath fading scenario.

Variations in the received signal power are due to three effects: mean propagation (path) loss, macroscopic (large scale or "slow") fading and microscopic (small scale or "fast") fading, which are demonstrated in Figure 8. The mean propagation loss is range dependent and results from absorption by water and foliage and the effect of ground reflection. Macroscopic fading results from the shadowing effect by buildings and natural features. Microscopic fading results from the constructive and destructive combination of multipath and is also known as fast fading since amplitude fluctuations are rapid when compared to macroscopic fading.

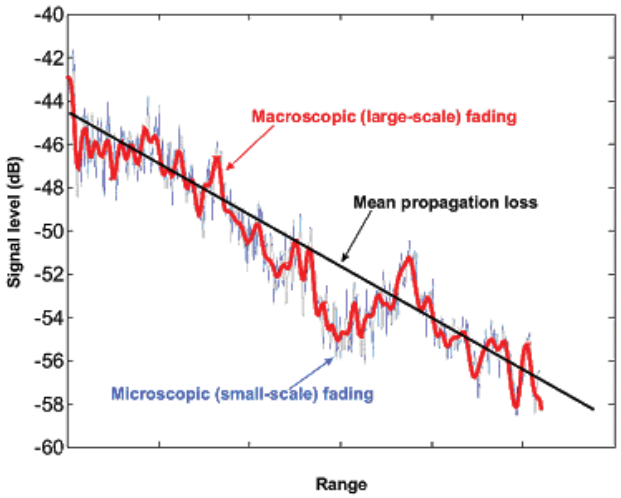

Figure 8. Signal power fluctuation versus range in wireless channel.

Multipath propagation results in the spreading of the signal over time and these time delays or "delay spread" cause frequency selective fading. Multipath is characterized by the channel impulse response and is modeled using a tapped delay line implementation. The characteristic of the tap variability is characterized by the Doppler spectrum. In addition to delay spread and Doppler spread, angular or angle spread is another important characteristic of the wireless channel. Angle spread at the receiver refers to the spread in Angles of Arrival (AoA) of the multipath components at the receive antenna array. Similarly, angle spread at the transmitter refers to the spread in Angles of Departure (AoD) for those multipath signals that finally reach the receiver. Angle spread causes spatial selective fading which means that signal amplitude depends on the spatial location of the transmit and receive antennas. When multiple antennas are applied to a wireless communication system, the various transmit-receive antenna pairs may have different channel impulse responses due to the spatial effects caused by angle spread, antenna radiation pattern and the surrounding environment. As MIMO operation requires low channel-to-channel correlation, it is important to understand how these spatial characteristics may influence system performance. In the next few sections of this application note there is a review of the basic characteristics found in any wireless channel, such as delay spread and Doppler spread, and in addition, the spatial effects will also be introduced as a means to create improved models for high performance channel emulators.

Wireless propagation characteristics

Mean propagation loss

The overall mean loss in signal strength as a function of distance will follow a $1/d^n$ law, where d is the distance between the transmitter and the receiver and n is the slope index ranging from a value of 2 to 6 depending on the environment. For example, in free space, n = 2 resulting in a 20 dB/decade slope. In a terrestrial environment, a typical value of n = 4 results in a 40 dB/decade signal loss as a function of distance. In this terrestrial setting, changing the distance from 100 feet to 1000 feet (one decade) would result in an average signal drop of 40 dB. Several empirically based path loss models have been developed for different propagation environments such as the models in COST-231[1] and ITU-R M.1225[2].

1. COST 231 TD (973) 119-REV 2(WG2). *Urban transmission loss models for mobile radio in the 900- and 1800-MHz bands*, September 1991.
2. *IEEE P802.11 WirelessLANs TGn channel models*, May 2004.

Macroscopic (slow) fading

Macroscopic or slow fading is caused by the shadowing effects of buildings or natural features and is determined by a local mean of the received signal over a distance of approximately 20 wavelengths. The macroscopic fading distribution is influenced by antenna heights, the operating frequency and the specific type of environment. The deviation of slow fading about the mean propagation loss is treated as a random variable that approaches a normal distribution when expressed in decibels (dB) and is considered to be log-normal as described by the following Probability Density Function (PDF).

$$f(x) = \frac{1}{\sqrt{2\pi}\sigma} e^{-(x-\mu)^2/\sigma^2}$$ *Equation 18*

In the above equation, x (in dB), is a random variable representing the large scale signal power level fluctuation. The variables, μ and σ, are the mean and standard deviation of x, respectively. Both μ and σ are expressed in dB. The mean value, μ, is equal to the mean propagation loss discussed in the previous section. The standard deviation, σ, may have values as high as 8 dB for some urban environments.

Microscopic (fast) fading

Microscopic or fast fading results from the constructive and destructive interference of numerous multipath signals received from the surrounding environment. Rapid changes in received signal strength may occur when the distance is varied by approximately one-half wavelength, thus giving this characteristic the name "fast" fading. When examining the fading statistics in the received power over a relatively short distance of approximately 20 wavelengths, the in-phase (I) and quadrature (Q) components of the superimposed signal can be modeled as an independent zero-mean Gaussian process. This model assumes that the number of scattered components is very large and independent. The voltage amplitude envelope of this received signal would then have a Rayleigh distribution with a PDF given by

$$f(x) = \begin{cases} \frac{x}{\sigma^2} e^{-x^2/2\sigma^2} & x \geq 0 \\ 0 & x < 0 \end{cases}$$ *Equation 19*

where x is a random variable taken here as the received voltage amplitude and σ is the standard deviation. A similar response would also be found for a stationary subscriber as a function of time due to the relative motion of scatterers in the local vicinity of the subscriber. The relative change in power level between a peak to null is typically 15-20 dB but can be as high as 50 dB under some channel conditions.

If there is a direct path present between transmitter and receiver, the signal envelope is no longer Rayleigh and the statistics of the signal amplitude follow a Rician distribution. Rician fading is formed by the sum of a Rayleigh distributed signal and a direct or Line-Of-Sight (LOS) signal. A fading environment associated with Rician statistics has one strong direct path reaching the receiver at roughly the same time delay as multipath from the local scatterers. The voltage amplitude envelope for a Rician distribution has a PDF given by

Equation 20

$$f(x) = \begin{cases} \frac{x}{\sigma^2} e^{\left(-\left(x^2+K^2\sigma^2\right)/2\sigma^2\right)} I_0\left(\frac{xK}{\sigma}\right) & x \geq 0 \\ 0 & x < 0 \end{cases}$$

where x is a random variable taken here as the received voltage amplitude and σ is the standard deviation. The term I_0 ( ) is the modified Bessel function of the first kind, order zero. Since I_0 ( ) = 1, the Rician distribution reduces to the Rayleigh distribution when K = 0. The Rician distribution is defined in terms of this K factor which for wireless environments is defined as the ratio of the power in the LOS component to the power in the scattered components.

As a measurement example showing the amplitude variation as a function of time for two independent channels in a SIMO system, the PXB was configured to create two independently Rayleigh-faded signals. Figure 9 shows the PXB measurement configuration screen of two parallel baseband generators that are independently faded using a Rayleigh distribution and the faded waveforms are connected to external RF signal generators for upconversion. As the channels use independent fading statistics, it is expected that their amplitude levels would be uncorrelated over time. Figure 10 shows the measurements of the amplitude for the two faded signals as a function of time. These measurements were obtained using an Agilent E4440A PSA-series spectrum analyzer set to "Zero-Span" mode. As shown in the figure, the two channels appear uncorrelated with each having separate fading nulls, some as deep as 45 dB.

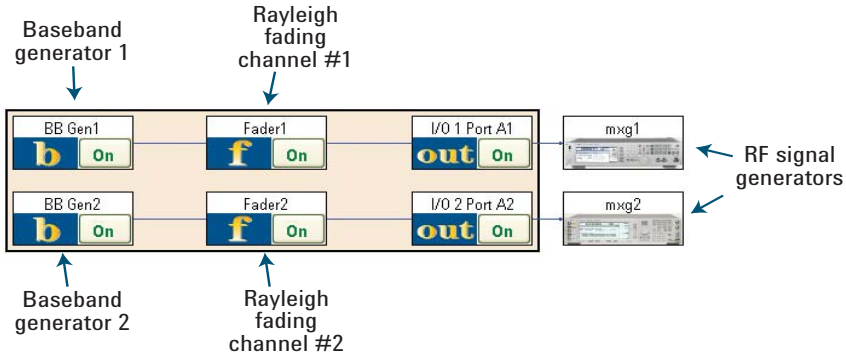

Figure 9. PXB setup screen for configuring two independent Rayleigh-faded channels using two signal generators.

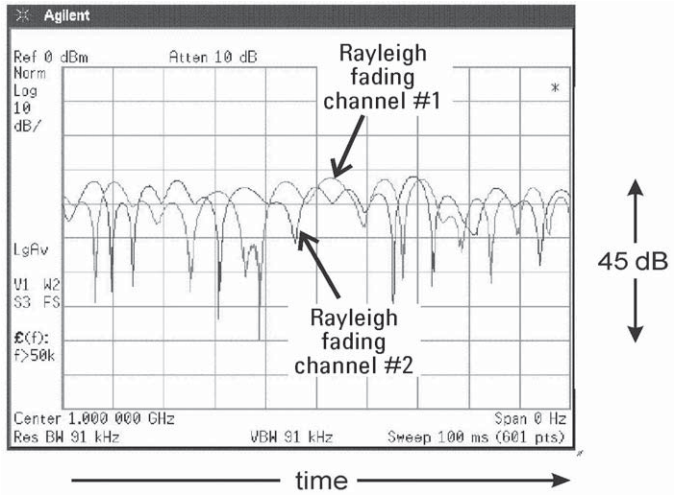

Figure 10. Received signal power as a function of time for two independent Rayleigh-faded channels.

Two of the primary performance criteria that are used to evaluate the Rayleigh fading performance of a channel emulator are the Cumulative Probability Distribution Function (CPDF) and the Level Crossing Rate (LCR). CPDF describes the probability of a signal level being less than the mean level. The LCR is the number of crossings per second relative to the mean signal power. For example, the 3GPP2 standard[1] recommends that the following test conditions and tolerances to the channel model parameters be supported by the channel simulator:

The requirement for CPDF is:

1) The tolerance shall be within ±1 dB of calculated, for power levels from 10 dB above to 20 dB below the mean power level.
2) The tolerance shall be within ±5 dB of calculated, for power levels from 20 dB below to 30 dB below the mean power level.

The requirement for LCR is:

The tolerance shall be within ±10% of calculated, for power levels from 3 dB above to 30 dB below the mean power level.

The theoretical and measured CPDF and LCR for the PXB are shown in Figure 11 and Figure 12, respectively. In these plots, the signal power is relative to the mean. The measured CPDF and LCR results track very well to the theoretical curves plots showing that the measured performance of the PXB exceeds the 3GPP2 standards for Rayleigh fading.

1. 3GPP2 standard for *Recommended Minimum Performance Standards for cdma2000® High Rate Packet Data Access Network*. More information available at **http://www.3gpp2.org/Public_html/specs/C.S0032-A_v1.0_051230.pdf**.

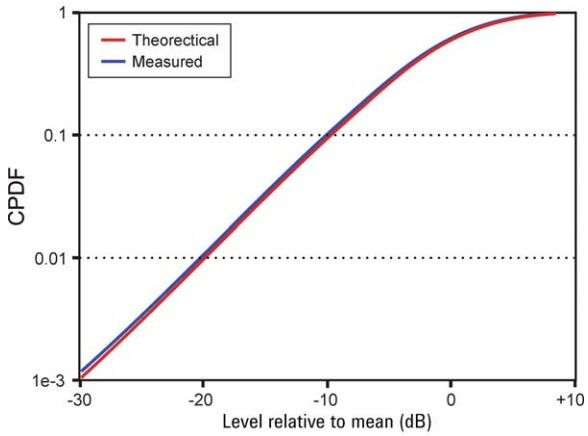

Figure 11. Theoretical CPDF versus measured CPDF.

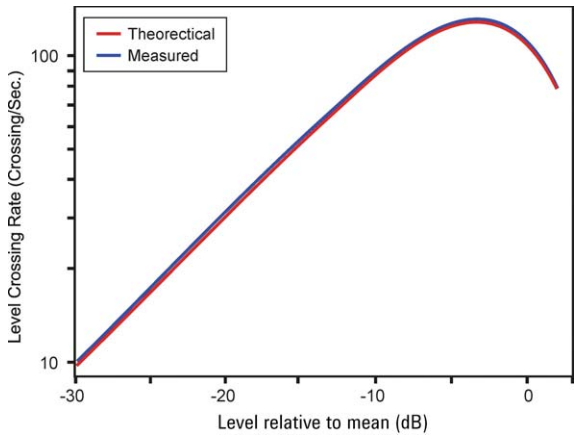

Figure 12. Theoretical LCR versus measured LCR.

Power delay profile (PDP)

In wireless communications, a signal transmitted to a receiver can arrive having traveled over many different paths through the radio channel. During transmission through the wireless channel, the signal may take the direct line of sight (LOS) path or may bounce off reflecting surfaces before arriving at the receive antenna. Since these multiple copies of the original transmitted signal travel different distances, they arrive at the receiver staggered in time and with different average power levels. The impulse response of the radio channel is used to characterize the predominant paths between the transmitter and receiver. Modeling the impulse response using a tapped delay line is a traditional technique for emulating a fading channel. In these models, each "tap" represents the sum of numerous multipath signals arriving at the same time. The tap amplitudes typically decrease over time as the signals arriving at later times have larger path loss and possibly undergo multiple reflections from the surrounding environment. At the receiver, the amplitude statistics for each tap may follow a Rician distribution if a LOS path is present or a Rayleigh distribution with the absence of the LOS path.

As depicted in Figure 13, the transmitter and receiver can be generalized as the foci of an ellipse, and any path bouncing from the same ellipse will have the same relative time delay. At a specific time delay, all the signals combine to form one tap in the channel impulse response. Each tap's mean power and delay is displayed as a channel impulse response also referred to as the Power Delay Profile (PDP). Figure 13 shows the PDP for a channel with three taps or signal paths. These three paths taken together form the wireless channel between the transmit antenna and the receive antenna. The PDP model serves as the basis for channel emulation as the fading instrument, such as the PXB, can be configured with the time delays and associated amplitude profile.

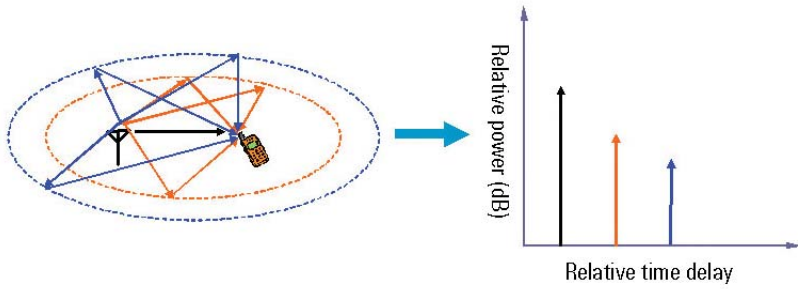

Figure 13. Channel impulse response using a three tap model for the PDP.

The PDP is the most significant characteristic for a wireless channel. Many wireless standards define which PDP profiles are required for system test. In addition, system performance is generally verified using other custom PDP profiles in order to stress the radio performance under a variety of multipath conditions. As a measurement example when using the PXB, a 2x2 MIMO channel was created and the PDP responses were measured for each of the four channels. Figure 14 shows the PXB block diagram for the 2x2 system configured with two baseband generators representing the Tx0 and Tx1 transmitters and 4 independent channels connecting the two transmitters to the two receivers. The figure also shows the PDP parameters for one of the fading channels. Each channel was identically configured with three Rayleigh-faded paths having a relative time delay of 0, 5μsec and 10μsec. The relative amplitudes for the three paths are –2.044 dB, –5.044 dB and –12.044 dB respectively.

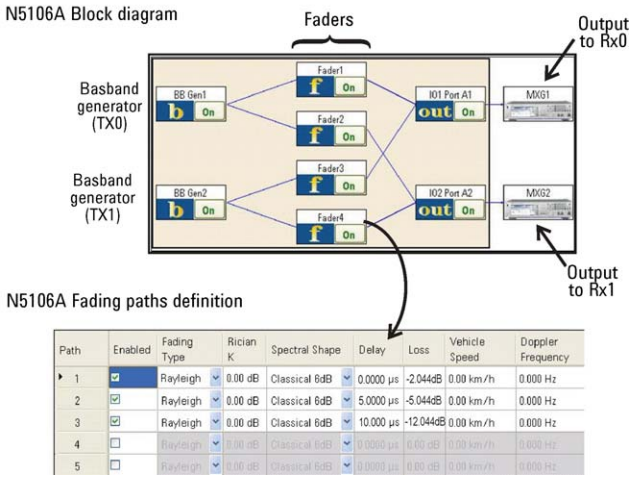

Path	Enabled	Fading Type	Rician K	Spectral Shape	Delay	Loss	Vehicle Speed	Doppler Frequency
1	☑	Rayleigh	0.00 dB	Classical 6dB	0.0000 µs	-2.044dB	0.00 km/h	0.000 Hz
2	☑	Rayleigh	0.00 dB	Classical 6dB	5.0000 µs	-5.044dB	0.00 km/h	0.000 Hz
3	☑	Rayleigh	0.00 dB	Classical 6dB	10.000 µs	-12.044dB	0.00 km/h	0.000 Hz
4	☐	Rayleigh	0.00 dB	Classical 6dB	0.0000 µs	0.00 dB	0.00 km/h	0.000 Hz
5	☐	Rayleigh	0.00 dB	Classical 6dB	0.0000 µs	0.00 dB	0.00 km/h	0.000 Hz

Figure 14. PXB setup for a 2x2 MIMO channel.

As a measurement example, Table 1 shows the measured path delays for each channel using the PXB configured as a 2x2 MIMO channel emulator. As shown in the table, the measured delays are almost identical to the desired values entered on the instrument. These values were obtained after averaging the channel impulse response over multiple sweeps. Table 2 shows the measured amplitudes for each path over the four channels. Once again, the PXB performance meets the strict requirements for accurately achieving the desired PDP channel response.

Table 1. Measured path delay and set values (Unit: ns)

	Channel Number				
Path Number	Channel 1	Channel 2	Channel 3	Channel 4	Set path delay value
Path 1	0.0	0.0	0.0	0.0	0.0
Path 2	4993.75	4995.0	4995.0	4987.5.0	5000.0
Path 3	9991.25	9992.5	9990.0	9981.25	10000.0

Table 2. Measured path loss and set values (Unit: dB)

	Channel Number				
Path Number	Channel 1	Channel 2	Channel 3	Channel 4	Set path power value
Path 1	–2.009	–2.131	–1.995	–2.122	–2.044
Path 2	–5.132	–4.864	–5.147	–4.892	–5.044
Path 3	–11.969	–12.107	–12.037	–12.053	–12.044

Fading Doppler spectrum

Time-varying fading due to scatter or the relative motion between the transmitter and receiver results in a spread in the frequency domain response often referred to as the Doppler spectrum. The Doppler spectrum results when a pure frequency tone spreads over a finite spectral bandwidth due to the relative motion between the transmitter and the receiver. The maximum Doppler frequency, $f_{d,max}$, is related to the relative velocity by the following equation.

$$f_{d,max} = f_c \frac{v}{c}$$ *Equation 21*

where v is the velocity of the mobile, f_c is the carrier frequency (Hz) and c is the constant for the speed of light. The spectral spreading of the pure tone would cover the range of $f_c \pm f_{d,max}$. The Doppler spectrum can be measured or calculated by the Fourier transform of the autocorrelation between the channel impulse response and the sinusoidal RF carrier. Assuming uniformly distributed scattering around a mobile terminal, there is an equal probability that the multipath signal is received with an arrival angle anywhere within the range from 0 to 360 degrees. In this case, the theoretical Rayleigh Doppler power spectrum would exhibit the classical "U-shape" as shown in Figure 15.

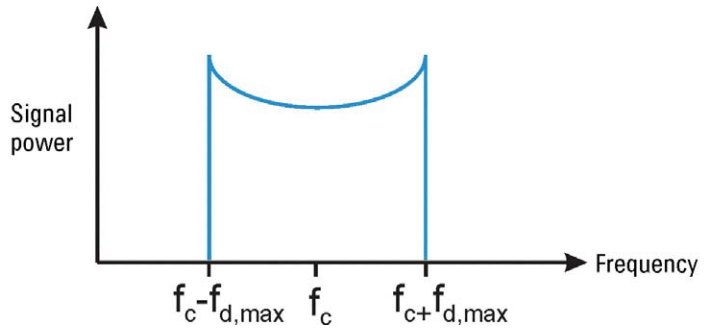

Figure 15. Theoretical Rayleigh Doppler spectrum.

Rician fading is formed by the sum of a Rayleigh distributed signal and a LOS signal. The Rician Doppler spectrum would then be the superposition of the Rayleigh Doppler spectrum and the resulting LOS Doppler. If there is relative motion between the transmitter and the receiver, then the LOS signal is subject to a static frequency shift related to the relative velocity. This Doppler shift for the LOS signal is determined according to the following equation.

$$f_{d,shift} = f_{d,max} \cos(\text{LOS AoA}) \qquad \textit{Equation 22}$$

Changing the LOS arrival angle will shift the Doppler frequency with respect to the center frequency up to a maximum frequency of $f_{d,max}$. The K factor for Rician fading affects the power level of the direct path relative to the multipath. Figure 16 shows the theoretical Doppler spectrum for Rician fading resulting from the summation of the Rayleigh Doppler spectrum and the LOS with a positive static frequency shift.

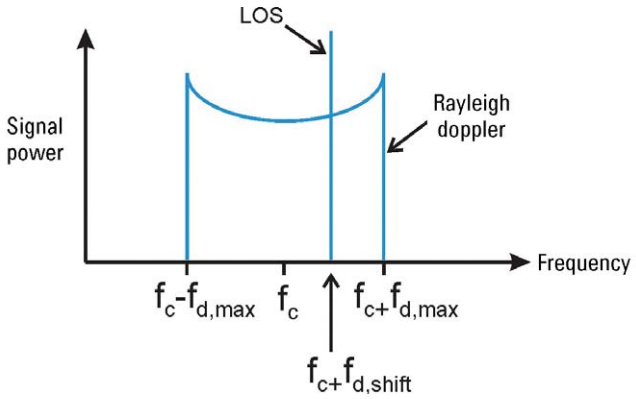

Figure 16. Theoretical Rician Doppler spectrum.

As discussed above, the power spectral density for Rayleigh and Rician fading describe the amplitude distribution as a function of frequency. However, several different frequency domain models can be used to represent the power spectrum shape produced by multipath effects and the relative motion between the transmitter and receiver. The PXB provides seven types of selectable spectrum shapes for accurate modeling of various multipath channels. Figure 17 shows Doppler spectrum of four standard models including the "classical 6 dB". The classical 6 dB spectrum is the most commonly used model and adheres to the spectral requirements detailed in numerous mobile communications standards for Rayleigh fading conditions. Other models not shown in Figure 17 include the Bell-Shape, Jakes-Classical and Jakes-Rounded.

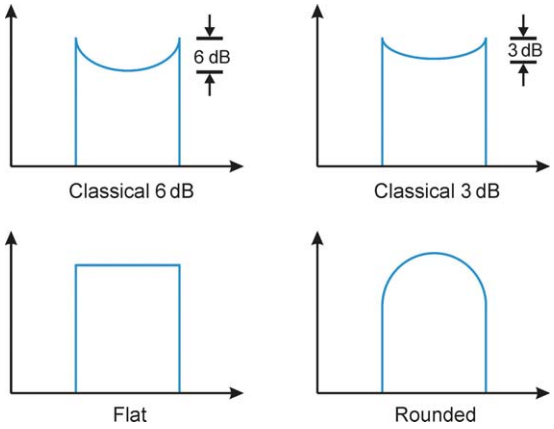

Figure 17. Fading power spectrum shapes.

As previously mentioned, the performance of Rayleigh fading implemented in a channel emulator such as the PXB, is often compared to a defined standard metric to ensure consistent operation. For example, the 3GPP2[1] standard recommends that the following Doppler conditions and tolerances be supported by the channel simulator. In the case when using a Rayleigh 6 dB Doppler spectrum, the measured power spectral density, S(f), around the RF carrier, fc will have maintained the following level of performance:

1) At frequency offsets |f-fc| = fd, the maximum power spectral density S(f) shall exceed S(fc) by at least 6 dB.

2) For frequency offsets |f-fc| > 2fd, the maximum power spectral density S(f) shall be less than S(fc) by at least 30 dB.

3) Simulated Doppler frequency, fd, shall be computed from the measured Doppler power spectrum. The tolerance on Doppler shall be ±5%.

1. 3GPP2 standard for *Recommended Minimum Performance Standards for cdma2000 High Rate Packet Data Access Network*. More information available at **http://www.3gpp2.org/Public_html/specs/C.S0032-A_v1.0_051230.pdf**.

The theoretical and measured Doppler power spectrum is shown in Figure 18. Here the Doppler frequency on the PXB was set to 120 Hz. The measured results demonstrate that the emulated Doppler spectrum performance can easily satisfy the recommended requirements. The computed Doppler frequency from the measured Doppler power spectrum is 121.23 Hz, resulting in a measurement error of 1.025%, which is well under the recommended ±5% tolerance.

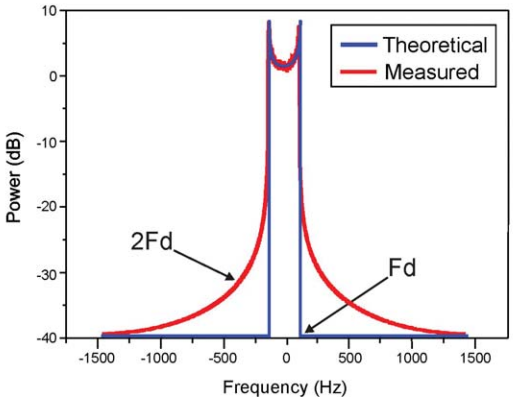

Figure 18. Rayleigh 6 dB theoretical spectral shape versus the measured spectral shape.

Dynamic fading

In mobile applications, the characteristics in the Power Delay Profile (PDP) would remain relatively constant over several meters. In this case the impulse response of a radio channel is averaged over this small distance to provide a "static" or wide sense stationary view of the channel conditions. As a mobile terminal moves over a wider area, the shape and characteristics of the PDP change dramatically as shown in the example in Figure 19.

Modern wireless communications systems must adapt to these dramatic changes to continuously mitigate the impact of multipath delay spread. To accurately evaluate the performance over a time-varying PDP, a fading emulator must be capable of emulating the time-varying changes in the paths delay characteristics. The sliding relative path delay and the Birth-Death time-varying relative path delay are two popularly employed models to emulate dynamic delay spread.

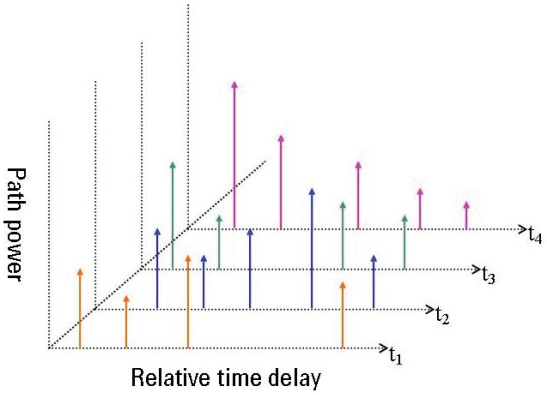

Figure 19. Dynamic fading characteristic showing the time-varying PDP.

Angle spread and Power Azimuth Spectrum

Traditional methods for modeling wireless channels, such as Power Delay Profile and Doppler spectrum, can accurately represent the multipath effects in a SISO system. The shortcoming of these traditional models is that they typically do not include spatial effects introduced by antenna position and polarization within the multipath environment. They also do not include the antenna pattern effects on the system performance. For example, in the simple MIMO case shown in Figure 20, the Tx0 transmit antenna, has two signal paths to the Rx0 receive antenna, namely, the LOS and one multipath. The LOS path leaves Tx0 with an angle of departure (AoD), θ_{d1}, measured relative to the array boresight as shown. The array boresight is defined as the normal (perpendicular) direction from the line of antenna array and it is primarily used as a reference point to describe angular direction. As the transmitter and receiver array boresight directions may not be pointing at each other, the received signals may arrive with a different angle defined as the Angle of Arrival (AoA). In Figure 20, the LOS path from the transmit antenna Tx0 arrives at the receive antenna, Rx0, with AoA of θ_{a1}. As shown in the figure, the AoD and AoD for the multipath between Tx0 and Rx0 are θ_{d2} and θ_{a2} respectively. For the signal paths connecting the Tx1 transmit antenna to Rx0, the associated AoDs and AoAs may be different from the Tx0 to Rx0 angles depending on the spatial separation of the Tx0 and Tx1 antennas. If the two transmit antennas are very close to one another, then the AoA and AoD would be very similar and a high fading correlation may exist between the antenna pairs (Tx0/Rx0 and Tx1/Rx0). As previously discussed, high correlation between transmit-receive antenna pairs reduces the performance for MIMO and STC systems. Therefore it is important for any MIMO channel emulator to include a model for the spatial effects and resulting channel correlations for the antenna pairs.

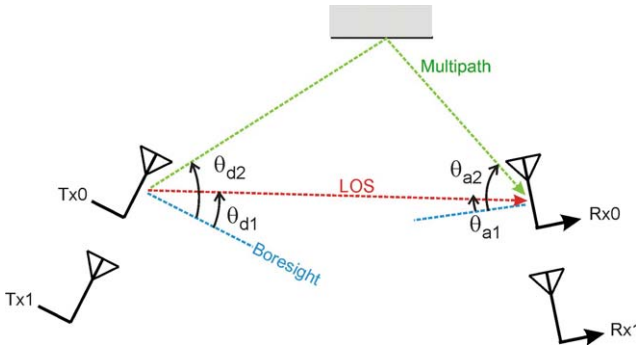

Figure 20. Spatial diagram for a 2x2 MIMO system showing the Angle of Departures (AoD) and Angle of Arrivals (AoA) relative to the transmit and receive antenna array boresight directions.

Rather than attempting to model each AoD and AoA in the channel emulator, an improved model for emulating the characteristics of a rich multipath environment can be achieved by including the spread of the AoDs and AoAs referred to as "angle spread". Angle spread causes spatial selective fading as the received signal amplitude depends on the spatial location of the antennas. When utilizing multiple antennas at the transmitter or/and receiver, the different transmit-receive antenna pairs may have different fading characteristics due to the antenna separations, the antenna radiation pattern and the surrounding environment. In the example shown in Figure 21, the angle spread for a typical Base Station (BS) is very narrow due to the fact that most scatterers are positioned far from the BS antennas. In contrast, the Mobile Station (MS) contains a large number of local scatterers surrounding the MS thus resulting in a very wide angle spread. If the BS antennas are placed physically close together, the narrow angle spread will result in high channel correlation. Fortunately, a BS often has the area to place its antennas far apart reducing the channel correlations. For MS with large angle spread, the antennas could be placed closer together while maintaining low channel correlations. Close antenna spacing is ideal for a mobile handheld that requires the placement of several antennas in a small package. Figure 21 also shows a tight grouping of spatial angles around the BS referred to as a "cluster". The cluster can be modeled by a mean angle surrounded by an angular spread. This representation allows a statistical PDF model to be applied to the power received as a function of angle.

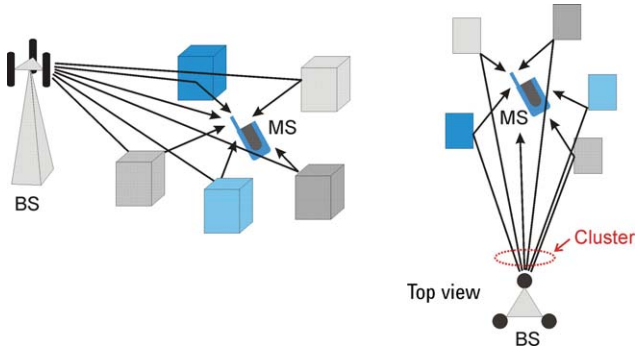

Figure 21. Diagram of angle spread as a function of antenna placement in a multipath environment.

The angle spread is characterized by the Power Azimuth Spectrum (PAS). Denoting the AoA or AoD by θ, the PAS of a signal, s(t, θ), represents the average power as a function of angle. Defined as $PAS(\theta) = E_{t|\theta}\,|s(t,\theta)^2|$ the distribution is normalized to satisfy the probability density function requirement as

$$\int_{-\pi}^{\pi} PAS(\theta)\,d\theta = 1 \qquad \textit{Equation 23}$$

Figure 22 shows three widely used PAS distribution models, Laplacian, Gaussian and Uniform, which are supported by the PXB. PAS distributions are typically selected based on the desired propagation environment, for example, the Laplacian model is suited for outdoor propagation in urban and rural areas[1, 2]. Each cluster is assigned a PAS distribution that best estimates the measured or modeled PAS for the wireless channel. The angle $\theta_{0,k}$ is the mean arrival/departure angle of the kth cluster. As shown in the figure, the Laplacian and Gaussian distributions are "truncated" to a value of $2\Delta\theta_k$ centered around the mean angle $\theta_{0,k}$. Table 3 shows the multimodal distribution functions for the uniform, Gaussian and Laplacian models for PAS.

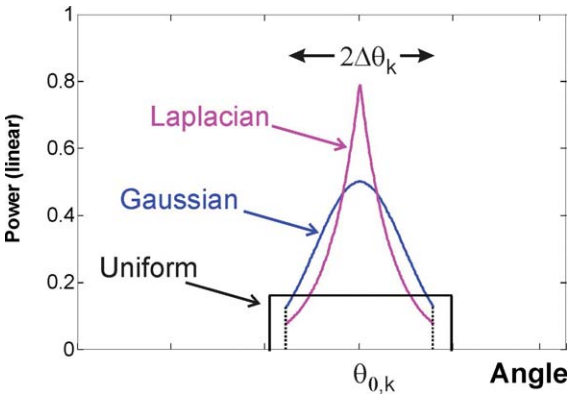

Figure 22. Power Azimuth Spectrum (PAS) distributions for modeling angular "clusters".

1. K. I. Pedersen, P. E. Mogensen, and B. H. Fleury, *Spatial channel characteristics in outdoor environments and their impact on BS antenna system performance*, in Proc. IEEE Vehicular Technology Conf. (VTC) 1998, Ottawa, Canada, vol. 2, pp. 719–723.
2. L. Schumacher, B. Raghothaman, *Closed-form expressions for the correlation coefficient of directive antennas impinged by a multimodal truncated Laplacian PAS*, IEEE Transactions on Wireless Communications, Vol. 4, No. 4, July 2005, pp. 1351-1359.

Table 3. Multimodal PAS distribution functions

Uniform	$PAS_U(\theta) = \sum_{k=1}^{Nc} Q_k S(\theta)$	*Equation 24*
Gaussian	$PAS_G(\theta) = \sum_{k=1}^{Nc} \frac{Q_k}{\sigma_k \sqrt{2\pi}} \exp\left[-\frac{(\theta-\theta_{0,k})^2}{2\sigma_k^2}\right] S(\theta)$	*Equation 25*
Laplacian	$PAS_L(\theta) = \sum_{k=1}^{Nc} \frac{Q_k}{\sigma_k \sqrt{2\pi}} \exp\left[-\frac{\sqrt{2}\lvert\theta-\theta_{0,k}\rvert}{\sigma_k}\right] S(\theta)$	*Equation 26*

The value for N_c shown in Table 3 above is the number of clusters, $\theta_{0,k}$ which is the mean arrival/departure angle of the kth cluster, and the constant Q_k is derived to fulfill the normalization requirement in Equation 23. The standard deviation, σ_k, in the Gaussian and Laplacian distributions are referred as Azimuth Spread (AS). The expression for $S(\theta)$ is related to the truncation of the distribution where the functions are only defined within a limited interval $[\theta_{0,k} - \Delta\theta_k, \theta_{0,k} + \Delta\theta_k]$ centered on the average angle $\theta_{0,k}$. Defining $U(\theta)$ as a step function, then the expression for $S(\theta)$ in Table 3 is defined as

$$S(\theta) = U\left[\theta - \left(\theta_{0,k} - \Delta\theta_k\right)\right] - U\left[\theta - \left(\theta_{0,k} + \Delta\theta_k\right)\right] \qquad \textit{Equation 27}$$

The notion of 'multimodal' for the distributions in Table 3 refers to conditions with more than one resolvable cluster, and whose spatial distribution can be modeled by a specific PAS function. For example, Figure 23(a) shows the measured PAS for a receiver operating in a relatively low multipath environment. The figure shows two high peaks representing two large clusters of multipath signals occurring between the transmitter and the receiver. Each cluster can be approximated by a PAS distribution using the best-fit to the actual distribution. For the example shown in Figure 23(a), the measured response is best approximated by two truncated Laplacian distributions centered on the two cluster peaks as shown in Figure 23(b).

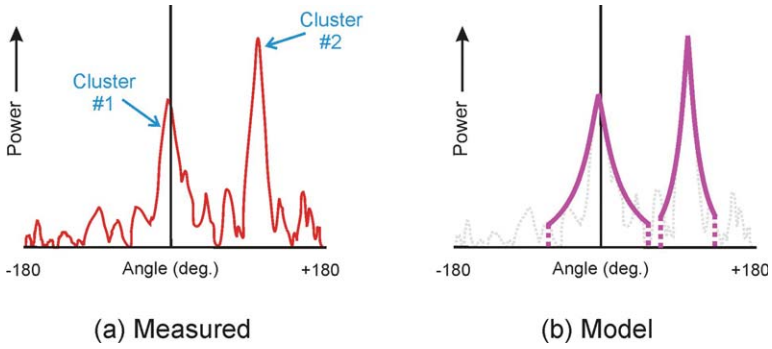

Figure 23. Measured PAS (a) and equivalent model (b) using Laplacian distribution.

The PXB can be used to easily define the cluster angles at the transmitter and receiver for each active path in the MIMO channel model. As shown in Figure 24, the PXB provides a table entry for the AoD, AoA and associated Azimuth Spread for each path within the selected channel. In this case, the PXB uses two path definitions in the channel each having a unique spatial distribution.

Path	d	Doppler Frequency	AOA	AOD	AoA Azimuth Spread	AoD Azimuth Spread	Phase Shift	Log Normal
3		6.667 Hz	51.16 °	15.31 °	68.00 °	5.00 °	0.00 °	☐
4		6.667 Hz	21.57 °	22.78 °	68.00 °	5.00 °	0.00 °	☐
5		6.667 Hz	123.34 °	21.75 °	68.00 °	5.00 °	0.00 °	☐
6		6.667 Hz	94.92 °	25.70 °	68.00 °	5.00 °	0.00 °	☐
7		6.667 Hz	19.19 °	22.61 °	68.00 °	5.00 °	0.00 °	☐

Figure 24. PXB configuration table for entering values of AoA, AoD and associated Azimuth Spread for modeling PAS effects in the wireless path.

The Power Azimuth Spectrum is just one spatial characteristic that may introduce correlations between the various MIMO channels. These spatially-induced channel correlations may also be effected by antenna pattern, spacing and polarization. These topics will be discussed in the next few sections of this application note and how they relate to the channel-to-channel correlation in a MIMO system.

Antenna gain and pattern

Antenna gain is a measure of the antenna's ability to direct radiated power into a particular direction. The antenna gain is typically quoted as a numeric value relative to a reference antenna where the reference antenna is usually taken as an ideal isotropic radiator that radiates equally in all directions. The antenna pattern describes the radiated power as s function of three dimensional space typically taken in spherical coordinates using ϕ and θ. In general, one horizontal cut through the spherical coordinates will provide the Azimuth pattern as a function of θ. This two-dimensional cut is typically displayed in either polar or rectangular coordinates. Antenna patterns typically fall into two categories - omni-directional and directive. The gain pattern for an omni-directional antenna is uniform in all directions. For the case of a dipole antenna positioned vertically (vertical polarization), the gain pattern is uniform in the azimuth plane as shown in the polar plot in Figure 25. In this example, the azimuth gain is constant for any angle from 0 degrees (boresight) to ±180 degrees. In a mobile application, an omni-directional antenna is preferred so that the user is not required to position or "point" the antenna for optimal SNR performance. In contrast, a directive antenna has a higher gain in the boresight direction as more of the radiated power is focused into that direction. Figure 25 also shows the gain pattern for a typical directive antenna. As shown in the figure, the directive antenna has higher gain in the boresight direction as compared to the omni-directional antenna. Directive antennas are often used in base station applications to divide the area surrounding the BS into sectors for improving coverage and reducing interference within the system.

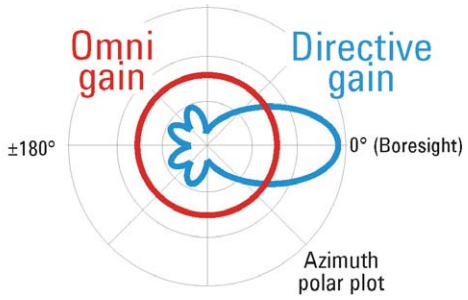

Figure 25. Typical gain pattern for omni-directional and directional antenna types.

In general, antenna patterns are normalized to their maximum field strength so that the displayed peak is set to 0 dB. The half-power or 3 dB beamwidth, θ_{3dB}, defines the angle for which the gain drops relative to the peak by 3 dB. For a three-sector base station antenna, the 3 dB beamwidth is typically equal to 70 degrees. For a six-sector base station antenna, the 3 dB beamwidth is equal to 35 degrees. In many cellular standards, the sectorized gain pattern is defined as

$$G(\theta) = -\min\left[\alpha\left(\frac{\theta}{\theta_{3dB}}\right)^2, \beta_m\right] \qquad \textit{Equation 28}$$

Where θ is defined as the angle between the direction of interest and the bore-sight of the antenna. The value for β_m is defined as the maximum attenuation and α is a constant. For the 3GPP standard[1], α is set to 12 dB. For a 3-sector antenna, $\theta_{3dB} = 70°$, $\beta_m = 20$ dB, and the resulting gain pattern in rectangular coordinates as a function of θ is shown in Figure 26. For a 6-sector antenna, $\theta_{3dB} = 35°$, $\beta_m = 20$ dB and the antenna pattern is also shown in Figure 26.

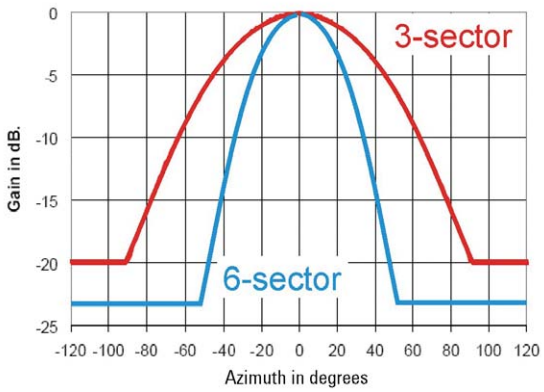

Figure 26. Gain pattern as a function of azimuth angle for 3-sector and 6-sector cellular antennas.

1. *Spatial channel model text description*, SCM-077 SCM-Text v2.0, November 20, 2002, pp. 7-10.

Antenna spacing

It can be shown that the antenna-to-antenna spacing at either the transmitter and/or receiver has a strong relationship to the overall spatial correlation. As the antenna spacing is reduced, one would expect that the channel-to-channel correlation would increase. In the extreme case, if the two transmit antennas were co-located with the same polarization, it would be expected that the channel characteristics to a single receive antenna would be identical. It is therefore important for the proper operation of a MIMO system that the antenna location be optimized for low channel-to-channel correlations. For example, Figure 27. shows two dipole antennas vertically oriented and spaced at a distance, d. Typically in a traditional phased array application, the antenna spacing is approximately $\lambda/2$ which is used to increase the gain of the composite array. In MIMO applications, the requirement is not for high array gain but rather for low channel-to-channel correlation. In this case the antenna spacing may be much larger than $\lambda/2$ with the only limitation being the area required to space the individual elements. For example, the mobile may select a a $\lambda/2$ spacing due to space constraints in a handheld device while a base station may use an antenna spacing of 4λ or more.

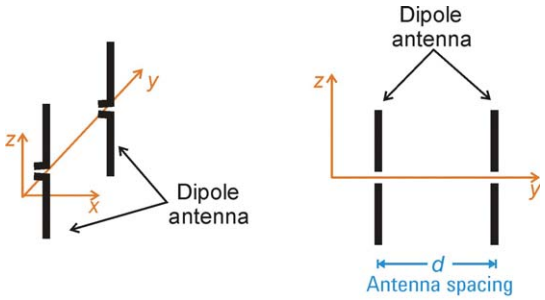

Figure 27. Dipole antenna placements with inter-element spacing equal to "d".

MIMO Channel Correlation

Spatial correlation

As MIMO systems require a rich multipath environment for proper operation, it is possible that the spatial positions of the multiple transmit antennas, relative to each other and relative to their placement in the surrounding environment, may give rise to high fading correlation between the different MIMO channels. The same conditions are also true for the antenna positions at the receiver. It will be shown in this section that inadequate antenna spacing leads to spatial correlation. The spatial correlation coefficient, ρ_{12}, between two antenna elements is a function of their spacing, the PAS, and the gain pattern of the individual elements. It is assumed that the antenna elements are identical with the same gain pattern. The correlation coefficient can be calculated using the following equation.

Equation 29

$$\rho_{12} = \frac{\int_{-\pi}^{\pi} e^{-j2\pi\frac{d}{\lambda}\sin(\theta)} PAS(\theta)G(\theta)d\theta}{\int_{-\pi}^{\pi} PAS(\theta)G(\theta)d\theta}$$

PAS(θ) is calculated using Equation 24, 25, or 26, dependent on the selection of the appropriate distribution, and "d" is the distance between antenna elements. The gain pattern, *G*(θ), is calculated using Equation 28 and assumes that the far field assumption holds and that the two antennas have exactly the same radiation pattern and boresight direction.

Figure 28 shows the absolute value of the correlation coefficient as a function of antenna spacing for several examples of antenna type and Azimuth Spread (AS). The antenna type was varied between "omni-directional" and directive using a "3-sector" antenna. Each curve represents a different value for AS covering 2, 5, 10, and 35 degrees. These curves assumed a single-modal Laplacian power azimuth spectrum with mean AoA=200 degrees and $\Delta\theta$ = 180 degrees. As expected, the correlation coefficient decreases for increasing normalized spacing and for increasing AS. It is also worthwhile to remark that for a given antenna spacing and large AS = 10 or 35, the directive antennas tend to be slightly more correlated than omni-directional ones.

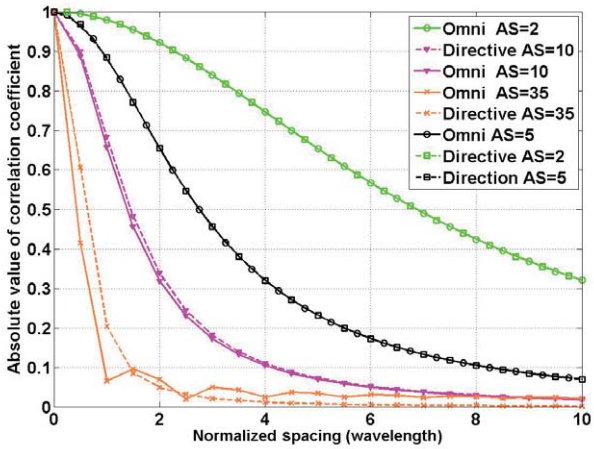

Figure 28. Relationship between antenna spacing and correlation coefficient using a Laplacian PAS with AoA = 200 degrees and $\Delta\theta$ = 180 degrees.

The spatial correlation matrix for the complete system can be calculated using Equation 29 and forming the individual spatial correlation matrices at the BS and the MS. For example, given a 2x2 MIMO system, assume the factors α and β represent the correlation coefficients, calculated using Equation 29, for the BS and MS antenna pairs, respectively. The correlation matrices for the BS and the MS are represented as

$$R_{BS} = \begin{pmatrix} 1 & \alpha \\ \alpha^* & 1 \end{pmatrix} \quad \textit{Equation 30}$$

$$R_{MS} = \begin{pmatrix} 1 & \beta \\ \beta^* & 1 \end{pmatrix} \quad \textit{Equation 31}$$

The system spatial correlation matrix for the downlink channel can be calculated using the Kronecker product

$$R_S = R_{BS} \otimes R_{MS} \quad \textit{Equation 32}$$

$$R_S = \begin{pmatrix} 1 & \beta & \alpha & \alpha\beta \\ \beta^* & 1 & \alpha\beta^* & \alpha \\ \alpha^* & \alpha^*\beta & 1 & \beta \\ \alpha^*\beta^* & \alpha^* & \beta^* & 1 \end{pmatrix} \quad \textit{Equation 33}$$

Antenna polarization correlation

In the previous section, it was shown that systems operating with a narrow range of angular spread may require antennas physically placed far apart in order to achieve low spatial correlation. Unfortunately some wireless devices tend to be physically small, thus limiting the antenna separation to under a wavelength depending on the frequency of operation. In some cases, an alternate solution is required to achieve the low channel-to-channel fading correlation required for MIMO operation. One technique to reduce the spatial correlation between two antennas is to "cross" polarize the antennas. In other words, position the antenna polarizations in orthogonal or near orthogonal orientations. As shown in Figure 29, two closely-spaced vertically-polarized (0/0) dipole antennas would have a high spatial correlation while orthogonally polarized (0/90) antennas, one vertical and one horizontal, would have a much lower correlation coefficient.

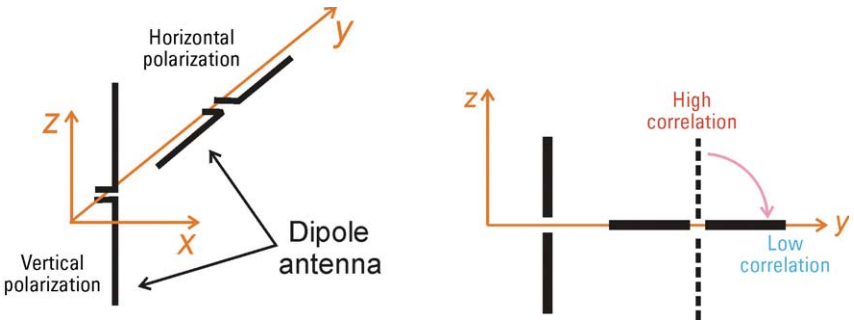

Figure 29. Diagram showing the effects of relative antenna polarization on the correlation characteristics.

The use of antennas with different polarizations at the transmitter and/or receiver may lead to power and correlation imbalances between the various MIMO channels. **The antenna polarization matrix**[1] is defined at the transmitter or receiver as

$$S = \begin{bmatrix} s_{vv} & s_{vh} \\ s_{hv} & s_{hh} \end{bmatrix}$$ *Equation 34*

where the index v represents vertical polarization and h horizontal polarization. The first index denotes the polarization at the transmitter and the second denotes the polarization at the receiver. Correlation between polarized antennas can be quantified using the Cross Polarization Ratio (XPR). The XPR is the power ratio between a pair of cross polarized antennas (v-h or h-v) to that of a co-polarized (v-v or h-h) case. Assume that the XPR = –8 dB, then

$$\frac{|s_{vh}|^2}{|s_{vv}|^2} = \frac{|s_{hv}|^2}{|s_{hh}|^2} = -8\ \text{dB}\left(=0.1585\right)$$ *Equation 35*

1. *MIMO channel model for TWG RCT Ad-Hoc Proposal*, V16, pp. 6-8.

For example, consider a 2x2 MIMO system. The BS polarization matrix with polarization angles $\alpha_1\alpha_2$ is

$$P_{BS} = \begin{bmatrix} \cos(\alpha_1) & \cos(\alpha_2) \\ \sin(\alpha_1) & \sin(\alpha_2) \end{bmatrix} \quad \textit{Equation 36}$$

The MS polarization matrix with polarization angles $\beta_1\ \beta_2$ is

$$P_{MS} = \begin{bmatrix} \cos(\beta_1) & \cos(\beta_2) \\ \sin(\beta_1) & \sin(\beta_2) \end{bmatrix} \quad \textit{Equation 37}$$

For the downlink case, the total channel polarization matrix is the matrix product of the BS polarization, channel polarization and MS polarization.

$$Q = P_{MS}{}^{T} S P_{BS} \quad \textit{Equation 38}$$

Lastly, the polarization correlation matrix is defined as

$$\Gamma = E\left\{ \mathrm{vec}(Q) \cdot \mathrm{vec}(Q)^{H} \right\} \quad \textit{Equation 39}$$

For specified polarization angles, such as +45/–45, 0/90 and 0/0, the diagonal elements of Γ have the same value, which means there is no power imbalance between different channels. For arbitrary polarization angles, the diagonal elements of Γ are not equal, which means that polarization leads to an undesired power imbalance between the channels.

Normalization of Γ is required so that the diagonal elements reflect the channels' power. In this case the correlation matrix then becomes

$$\Gamma^{R} = \frac{K}{\sum_{i=1}^{K} \Gamma_{i,i}} \Gamma \quad \textit{Equation 40}$$

This power normalization process is based on the assumption that the overall channel power is $K = N_r N_t$ for a MIMO system with N_t transmit antennas and N_r receive antennas. The correlation matrix Γ^R will properly reflect the channel imbalance due to polarization, and the diagonal elements in Γ^R relate to the relative power in each channel.

Using a 2x2 MIMO channel as an example, assume that the XPR= –8 dB and the system uses cross-polarized MS antennas (0/90) and slant-polarized BS antennas (+45/–45). The resulting polarization correlation matrix is

$$\Gamma^R = \begin{bmatrix} 1 & 0 & 0.7264 & 0 \\ 0 & 1 & 0 & -0.7264 \\ 0.7264 & 0 & 1 & 0 \\ 0 & -0.7264 & 0 & 1 \end{bmatrix}$$

Equation 41

The diagonal elements of this polarization correlation matrix are all ones, which show that the selected polarization angles do not result in a power imbalance among the different MIMO channels. The other elements in the matrix relate to the correlation between different channels. For example, in the first row, this matrix shows that channel 1 is only correlated to channel 3 with a coefficient of 0.7264. The second row shows that channel 2 is only correlated with channel 4. It can be shown that the use of antennas with differing polarizations at the transmit and receive leads to polarization diversity.

As another example, consider a case where the correlation matrix results in a power imbalance. Here, assume that the antenna polarization angles are –10/80 at MS antenna and +30/–60 at BS. The resulting polarization correlation matrix is

$$\Gamma^R = \begin{bmatrix} 1.3413 & 0.1242 & 0.5911 & 0.2151 \\ 0.1242 & 0.6587 & 0.2151 & -0.5911 \\ 0.5911 & 0.2151 & 0.6587 & -0.1242 \\ 0.2151 & -0.5911 & -0.1242 & 1.3413 \end{bmatrix}$$

Equation 42

For this matrix, the diagonal elements are not equal and they demonstrate that using this combination of polarization angles leads to a power imbalance among the different channels.

Combined spatial and antenna polarization correlation

It is known that spatial and polarization correlation effects in compound antenna systems are independent and multiplicative. In this case, the corresponding spatial and polarization correlation matrices can be derived separately and combined by an element-wise matrix product. The combined spatial-polarization correlation matrix is then defined as

$$R = R_S \cdot \Gamma^R \qquad \textit{Equation 43}$$

where R_s is the system spatial correlation matrix calculated using Equation 33 and Γ^R is the polarization correlation matrix calculated using Equation 40.

Orthogonal antenna positions (0/90) provide the lowest spatial correlation but may not always be required or practical under all conditions. For example, the diagrams in Figure 30 show two possible 2x2 MIMO configurations for base station and mobile antenna positioning. In one case, as shown in Figure 30(a), all the antennas are vertically polarized resulting in a potentially high level of spatial correlation. To overcome this problem, the BS antennas are spaced at 4λ to improve the correlation for this typically narrow angle spread condition. The spacing at the MS is fixed at $\lambda/2$. This first case is the reference antenna configuration for the high correlation channel model as specified in the WiMAX standard. For this high correlation condition, all the antennas have the same polarization angle, which does not provide any polarization diversity. Therefore the polarization matrix is defined as

$$\Gamma^R = \begin{pmatrix} 1 & 1 & 1 & 1 \\ 1 & 1 & 1 & 1 \\ 1 & 1 & 1 & 1 \\ 1 & 1 & 1 & 1 \end{pmatrix} \qquad \textit{Equation 44}$$

By applying Equation 43 to this high correlation antenna configuration, the combined spatial-polarization correlation matrix is the same as the spatial correlation matrix previously defined in Equation 33.

$$R = R_S \cdot \Gamma^R = \begin{bmatrix} 1 & \beta & \alpha & \alpha\beta \\ \beta^* & 1 & \alpha\beta^* & \alpha \\ \alpha^* & \alpha^*\beta & 1 & \beta \\ \alpha^*\beta^* & \alpha^* & \beta^* & 1 \end{bmatrix} \qquad \textit{Equation 45}$$

The second case, as shown in Figure 30(b), has the antennas at the BS polarized at ±45-degree orientations while the mobile uses orthogonal polarization (0/90). This second combination can greatly reduce the channel-to-channel correlation required for the proper operation of the MIMO system. This combination is the reference antenna configuration for the low correlation channel model in the WiMAX standard. For this configuration, the polarization matrix was defined in Equation 41 and the final correlation matrix for this antenna configuration is defined as

$$R = \begin{bmatrix} 1 & 0 & \gamma\alpha & 0 \\ 0 & 1 & 0 & -\gamma\alpha \\ \gamma\alpha^{*} & 0 & 1 & 0 \\ 0 & -\gamma\alpha^{*} & 0 & 1 \end{bmatrix} \qquad \textit{Equation 46}$$

where $\gamma = 0.7264$.

Comparing the two correlation matrices found in Equations 45 and 46, it can be concluded that introducing different polarization angles at the BS and MS will lower the channel-to-channel correlations.

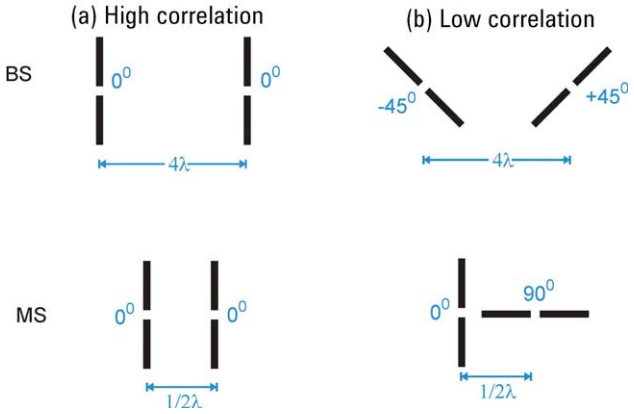

Figure 30. BS and MS antenna configurations for (a) high and (b) low channel correlations.

Configuring the channel emulator for spatial correlation

It is often desired to improve the process of entering the correlation matrices into a wireless channel emulator while minimizing the mathematical complexity and still be capable of modeling realistic wireless channels. The PXB greatly improves the process of MIMO channel emulation by eliminating the need to calculate complex correlation matrices and allowing the user to enter the physical antenna characteristics directly in the instrument. For example, Figure 31 shows the PXB user interface for entering the receive channel (Rx) spatial parameters including antenna type and spacing. A similar table is used to enter the transmit antenna parameters using the same menu. The PXB uses this spatial information along with the AoAs and AoDs entered in the fading paths table, shown in Figure 24, to automatically calculate the spatial-polarization correlation matrix. This simple entry table eliminates the burden for calculating the correlation matrices and manually entering the coefficients into the emulator.

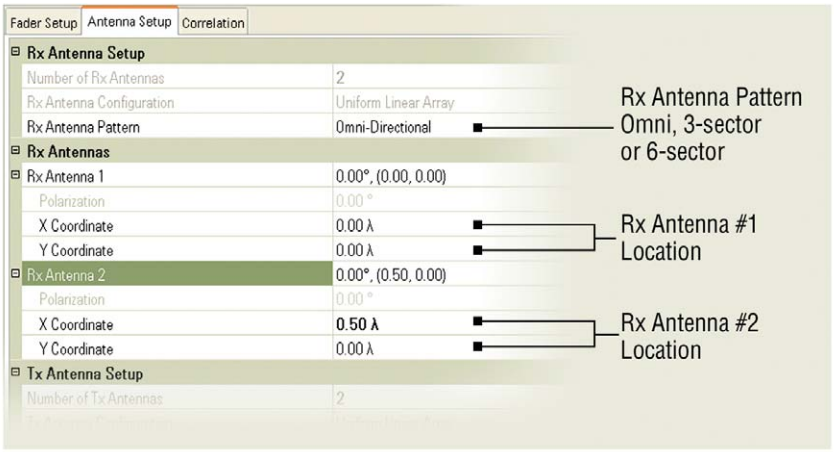

Figure 31. PXB antenna parameter setup screen.

Correlation property validation

The correlation property among different channels is a unique characteristic for MIMO systems. As previously discussed, correlation between MIMO channels may have a negative effect on the ability to separate the multiple data streams at the MIMO receiver. A high-performance channel emulator must provide correlation characteristics when compared with a traditional SISO channel emulator. It is also important to validate the channel emulator's performance by measuring the correlation matrix produced in comparison with the instrument's configuration. As a measurement example, the PXB is configured with a three-path 2x2 MIMO channel using cross-polarized (0/90) MS antennas and slant-polarized (–45/45) BS antennas similar to the conditions in Equation 41, above. Table 4 shows the correlation matrix for the configured system. The measured correlation matrices for paths 1 through 3 are shown in Table 5.

Table 4. Desired correlation matrix for the 2x2 MIMO channel

1	0	0.7264	0
0	1	0	–0.7264
0.7264	0	1	0
0	–0.7264	0	1

Table 5. Measured correlation matrix as a function of path

Measured correlation matrix for Path 1 is:

1	0.005	0.693	0.025
0.005	1	0.004	–0.732
0.693	0.004	1	0.023
0.025	–0.732	0.023	1

Measured correlation matrix for Path 2 is:

1	0.014	0.704	0.008
0.014	1	0.009	–0.742
0.704	0.009	1	0.005
0.008	–0.742	0.005	1

Measured correlation matrix for Path 3 is:

1	0.026	0.687	0.007
0.026	1	0.004	–0.728
0.687	0.004	1	0.014
0.007	–0.728	0.014	1

The measured results are very consistent with the correlation coefficients desired for this configuration. As a result, the PXB does an excellent job of creating MIMO channels with a desired amount of spatial correlation that simulates real-world test conditions.

Per-path correlation versus per-channel correlation

When standardizing test conditions for emulating MIMO channels, the correlation properties can be “per-path” or “per-channel”. Per-path correlation means each tap uses a different correlation matrix, while per-channel correlation means all the taps use same correlation matrix. As shown in Equation 34, the spatial correlation coefficient between two antenna elements is a function of antenna spacing, the PAS, and the radiation pattern of the antenna elements. The PAS is a function of path AoA/AoD, and path AS. In real-world conditions it is not universal that all the paths have the same AoA/AoD and AS values, therefore different paths could have different correlation coefficients. The use of per-path correlation may improve the channel emulation performance. In order to emulate this real-world scenario, the MIMO channel models used for Mobile WiMAX and the WLAN 802.11n standards use the per-path correlation based on different AoA/AoD for each path. While per-path spatial correlation can closely model a real wireless channel, it has a high level of computational complexity. Fortunately, the PXB has pre-defined channel models to automatically configure the instrument’s path correlations.

Some wireless standards such as LTE, in an effort to reduce the model’s complexity, have recommended the per-channel correlation model without considering the path AoA/AoD information. When testing a MIMO system against these specifications, the PXB can also provide per-channel correlations using pre-defined models, or, as shown in Figure 32, provide a simple table entry for custom per-channel emulation models.

When emulating wireless channels it is important to understand the test requirements for spatial correlations. Fortunately the PXB has the flexibility to support both per-path correlation and per-channel correlation, either individually or at the same time.

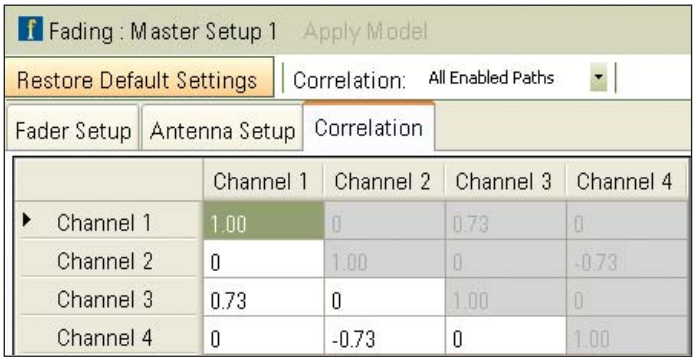

Figure 32. PXB “per-channel” correlation setup screen.

Theoretical MIMO channel capacity

In order to give a more intuitive impression of channel capacity loss caused by fading correlation, Figure 33 compares the capacity as a function of SNR for a 2x2 MIMO system with different correlation coefficients at the transmitter (α) and the receiver (β). Compared with the completely independent MIMO channel ($\alpha = \beta = 0$), the figure shows that there is a little capacity loss for the low correlated channels ($\alpha = \beta = 0.3$). For highly correlated channels ($\alpha = \beta = 0.95$) at high SNR, the capacity decreases by 3.9 bps/Hz as compared to the ideal uncorrelated case. For completely correlated channels ($\alpha = \beta = 1.0$), the capacity decreases by 4.4 bps/Hz at high SNR. Note that even when the correlation coefficients are 1, there is still an increase in capacity relative to SISO, though the improvements are small, by increasing the number of antenna pairs. The largest improvements are achieved when the channels are independent. In this case, the MIMO capacity is improved by, approximately, the SISO capacity multiplied by $\min(N_t, N_r)$[1]. Appendix A provides additional details for the theoretical derivation of the MIMO channel capacity.

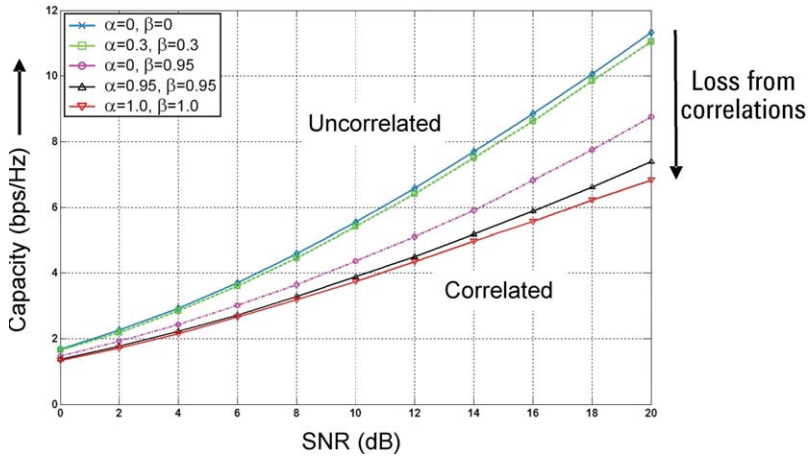

Figure 33. Ergodic capacity for a 2x2 MIMO system with different transmit and receive correlation coefficients.

1. C. Chuah, D. Tse, J. Kahn and R. Valenzuela, *Capacity scaling in MIMO wireless systems under correlated fading*, IEEE Trans. Inf. Theory, 48(3), 637-650, March 2002.

Configuring the channel emulator to achieve the desired correlation

Under ideal conditions, MIMO systems provide dramatic channel capacity gain through increased spatial diversity. As previously shown however, the capacity gain is reduced if the fading characteristic among various channels is correlated. Many wireless standards, such as WiMAX and LTE, recommend test scenarios that use correlated channel matrices. One approach that is widely accepted for defining the correlation properties of a MIMO channel relies on the "λ-parameter". In this case, λ provides an indication of the correlation as it relates to capacity. The capacity, operating under a specified SNR, is defined as a linear interpolation of the capacity for a completely correlated MIMO channel to that of an uncorrelated MIMO channel. Using the λ-parameter, the resulting capacity is defined as

$$C_\lambda = (1-\lambda)\,C_0 + \lambda C_1 \qquad \textit{Equation 47}$$

where C_0 is the channel capacity without correlation and C_1 is the channel capacity when the channels are completely correlated. With this approach, it is simple to specify the expected correlation degree through the λ-parameter. For example, in LTE channel model for 2x2 antenna configurations, the medium and high correlation matrices are defined using values of $\lambda \approx 0.5$ and $\lambda \approx 0.9$, respectively. For a system operating with a target value for λ and under a specified SNR, the correlation matrix can be tuned to achieve the desired correlation.

The correlation matrix that can guarantee the expected capacity, C_{λ}, is not unique, and different correlation matrices can be chosen to satisfy this capacity requirement. One very flexible method to achieve the desired correlation matrix is to adjust the antenna configuration, such as element spacing and/or polarization. As an example, the BS antenna spacing is adjusted using a 2x2 MIMO configuration with vertically polarized antennas, as shown in Figure 30(a), until the desired correlation is achieved. The antenna parameters for the MS are fixed with values shown in Table 6. The receiver correlation coefficient, β, is calculated using Equation 29.

Table 6. MS (Receiver) antenna configuration

	Antenna spacing in wavelength	Antenna type	AS (degrees)	AoA (degrees)	Correlation coefficient (β)
MS	0.5	Omni	35	67.5	–0.6905 + 0.3419i

For this example, the BS uses a 3-sector antenna configuration with AS=2 degrees and AoD = 50 degrees. The BS correlation coefficient, α, changes when adjusting the spacing between the BS antenna elements. Under this configuration, the combined spatial-polarization correlation matrix can be calculated using Equation 45. If the calculated channel capacity is lower than the desired channel capacity, the antenna spacing is increased to reduce the correlation and thus increase the channel capacity. By iteratively adjusting the antenna spacing, the desired λ can be achieved. Table 7 shows correlation index λ as a function of BS antenna spacing for this 2x2 MIMO example.

Table 7. Relationship between BS antenna spacing, correlation coefficient and channel capacity under specified SNR values

Antenna spacing d	Correlation coefficient α	λ SNR = 10 dB	λ SNR = 20 dB
0	1.0000	0.9060	0.9445
0.5	–0.7390 + 0.6700i	0.9004	0.9270
1.0	0.0969 - 0.9854i	0.8921	0.8806
1.5	0.5827 + 0.7857i	0.8543	0.8189
2.0	–0.9433 - 0.1881i	0.8252	0.7598
3.0	–0.2687 + 0.8779i	0.7591	0.6542
4.0	0.7955 + 0.3350i	0.6958	0.5636
5.0	0.3854 - 0.7028i	0.6246	0.4951
6.0	–0.6061 - 0.4196i	0.5704	0.4389
7.0	–0.4388 + 0.5106i	0.5232	0.3971

Applying SNR to MIMO channels

A convenient place for setting the channel's Signal to Noise Ratio (SNR) is typically at the receiver. The signal power can be accurately measured with a power meter and the channel emulator can generate the required noise according to the desired SNR. This technique is valid for SISO systems and MIMO systems that have uncorrelated channels. When the MIMO channels are correlated, an alternate approach for measuring the signal power and generating noise is required.

SNR for SISO and uncorrelated MIMO channels

For SISO systems, the received signal, Y, is defined as

$$Y = HX + N \qquad \textit{Equation 48}$$

where X is the transmitted data, H is the channel coefficient and N is the noise. For a specified SNR, the signal power, S, is first measured at the output of the channel emulator in the absence of noise. The covariance of the noise, σ^2, being a random Gaussian process, can be calculated and added by the channel emulator to simulate the effect of applying SNR to the SISO channel. As shown in Appendix B, this technique is also valid for uncorrelated MIMO channels. In this case, the signal at the receiver can also be defined using Equation 48 where X is now a vector of M_t transmitted signals, H is the channel coefficient matrix with M_r rows and M_t columns, and Y is a vector of M_r received signals. In the MIMO case, N is an M_r row of random Gaussian processes. It is also shown in Appendix B that the signal power can be measured at either the receiver or the transmitter for the uncorrelated MIMO system.

SNR for correlated MIMO channels

When the MIMO channels are correlated, the measured signal power at the receiver side can be dependent on the correlation of the channels. This correlation dependency prevents a channel emulator from accurately configuring the MIMO system for a desired SNR, using power measurements at the receiver. To overcome this difficulty, the channel emulator can use measurements of the signal power at the transmitter to appropriately set the required SNR. The following derivation shows a simplified example using a 2x1 MISO system to demonstrate an appropriate measurement technique for configuring the SNR in a channel emulator when the channels are correlated.

The MISO pre-coding matrix is defined as

$$\frac{1}{\sqrt{2}}\begin{bmatrix}1\\ e^{j\theta}\end{bmatrix} \qquad \textit{Equation 49}$$

The signal transmitted from antenna 1 is $\frac{X}{\sqrt{2}}$, the signal transmitted from antenna 2 is $\frac{Xe^{j\theta}}{\sqrt{2}}$, and the transmitted signal power from each antenna is S. The channel between transmit antenna 1 and the receive antenna is H_1. The channel between transmit antenna 2 and the receive antenna is H_2. Using Equation 48, the received signal becomes

$$Y = \frac{X}{\sqrt{2}}H_1 + \frac{Xe^{j\theta}}{\sqrt{2}}H_2 \qquad \textit{Equation 50}$$

If H_1 is independent with H_2, the received signal power is

$$E(YY^*) = (\overline{H}_1 + \overline{H}_2)S \qquad \textit{Equation 51}$$

where $\overline{H}_1$ and $\overline{H}_2$ represent average channel gains of H_1 and H_2 respectively. When $\overline{H}_1 = \overline{H}_2 = \overline{H}$, then $E(YY^*) = 2\overline{H}S$.

If H_1 is completely correlated with H_2, meaning that $H_1 = H_2 = H$, then the received signal becomes

$$Y = (1 + e^{j\theta})H\frac{X}{\sqrt{2}} \qquad \textit{Equation 52}$$

and the received signal power is

$$E(YY^*) = 2(1 + \cos(\theta))\overline{H}S \qquad \textit{Equation 53}$$

When $\theta = \pi/4$, the received signal power becomes $2(1 + \sqrt{2}/2)\bar{H}S$, which is different from the case with independent channel conditions. Therefore if the measured signal power at receiver is used to calculate the noise power required for a specific SNR value, then the added noise power will vary according to the fading correlation property. Continually adjusting the noise power as a function of correlation property introduces unnecessary complexity into the measurement and may result in reduced accuracy when configuring the measurement SNR. To overcome this difficulty, the PXB defines the SNR relative to the transmitted signal power and uses the following SNR definition

$$SNR = \frac{S_1\overline{H}_1 + S_2\overline{H}_2}{\sigma^2}$$ *Equation 54*

where S_1 and S_2 are the signal powers from each transmitter. With this definition, the PXB measures the signal power at the transmitters prior to fading and then adds the appropriate noise power to achieve the desired SNR. In this technique the noise contribution can be determined without considering the fading correlation property of the channel. Additional information regarding SNR in correlated MIMO channels is provided in Appendix B.

Configuring SNR using the PXB

The complexity of controlling and calibrating the signal power and noise power in a MIMO test are eliminated when using the PXB. The PXB uses automated signal routing and power calibration to precisely control the SNR in each channel of the MIMO setup. Figure 34 shows the PXB menu for entering the required SNR over the desired integration and noise bandwidths. The integration bandwidth (BW) is typically set to the channel bandwidth of the MIMO receiver. The noise power is usually spread over a wide bandwidth but is calibrated over the integration BW when calculating SNR, see Figure 35.

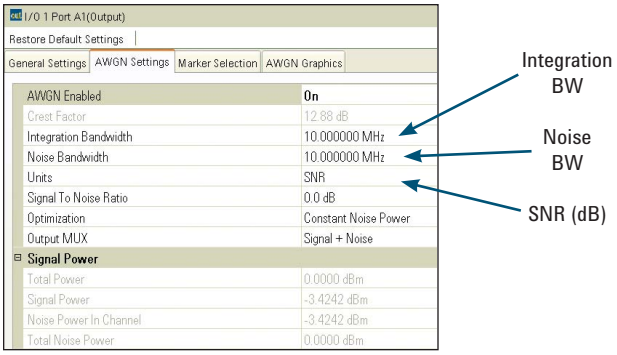

Figure 34. AWGN settings using the PXB.

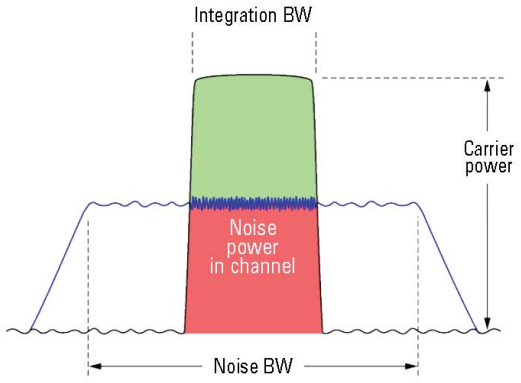

Figure 35. Signal and noise bandwidth definitions.

Configuring Standard-Compliant MIMO Channels using the PXB

Configuring custom correlation matrices targeted for a specific application can be a lengthy process. Fortunately, the PXB provides a set of pre-defined MIMO channel models based on the specifications of several wireless standards including Mobile WiMAX and LTE. The instrument is configured using a simple menu structure for selecting the channel model. In addition, custom correlation matrices and path definitions may be created and saved using the instrument's interface as shown in Figure 36.

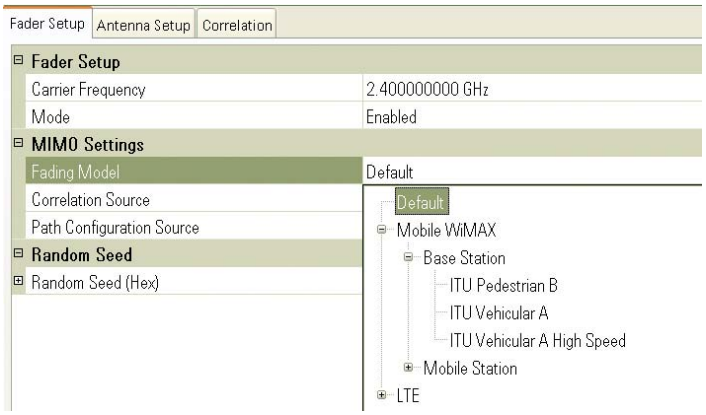

Figure 36. PXB fading model selection menu.

For signal generation, the PXB has up to 4 built-in baseband generators allowing the creation of standard-compliant signals with support for up to 4x2 MIMO in one instrument. The baseband generators can also play back waveforms created by the Agilent Signal Studio[1] software tool which provides an extensive library of standard-compliant and specialized waveforms.

1. For more information about Agilent Signal Studio, visit **www.agilent.com/find/signalstudio**.

The PXB can be configured to fade RF signals with the addition of MXA signal analyzers, for downconverting and digitizing the RF signal for real-time fading inside the PXB. For example, Figure 37 shows the PXB configuration block diagram for a 2x2 MIMO system with RF fading using two MXA signal analyzers. For this configuration, the PXB connects the faded signals to MXG signal generators for upconversion back to RF.

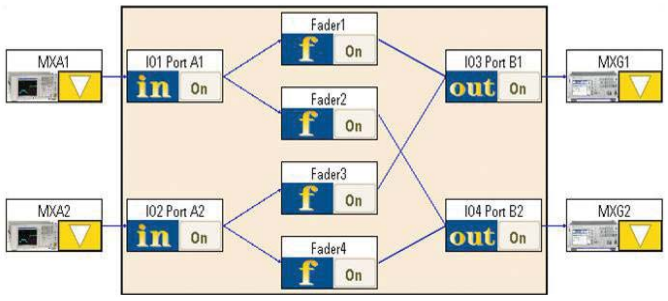

Figure 37. PXB configuration block diagram for RF-to-RF fading of a 2x2 MIMO signal.

The PXB hardware can be configured with up to 12 DSP blocks. Each DSP block can be configured as a baseband generator with 512 Msamples of playback memory or as a real-time fader with up to 24 paths. The flexibility in configuring the channel hardware allows up to 4 baseband generators to be used with up to 8 faders. The DSP blocks deliver modulation and fading bandwidths up to 120 MHz. The PXB can also sum up to 4 baseband generators for interference and mixed-modulation testing. Power and noise calibration is quickly and accurately performed by the PXB eliminating the need for complicated and lengthy system calibrations. The PXB supports analog and digital I/Q output connections to numerous N5102A digital signal interface modules and Agilent RF signal generators. It also supports RF inputs from MXA signal analyzers.

The flexibility of the PXB to support RF, analog and digital interfaces for signal generation and real-time fading of MIMO signals delivers an advanced test capability when developing and validating components and systems for current and emerging wireless systems.

Related Literature

Agilent Application Note, *Concepts of High Speed Downlink Packet Access: Bringing Increased Throughput and Efficiency to W-CDMA*, Literature number 5989-2365EN, January 18, 2007

Agilent Application Note 1509, *MIMO Wireless LAN PHY Layer [RF] Operation & Measurement*, Literature number 5989-3443EN, September 16, 2005

Agilent Application Note 1578, *IEEE 802.16e WiMAX OFDMA Signal Measurements and Troubleshooting*, Literature number 5989-2382EN, June 6, 2006

Appendix A: Theoretical Model for MIMO Channel Capacity

The wireless channel can be modeled as a linear time-varying system by using $h(\tau_k, t)$ to define the channel impulse response at time t and delay τ_k, where $k = 0, ..., L - 1$ and L is the multi-path number. Denoting the impulse response between the jth transmit antenna and the ith receive antenna by $h_{i,j}(\tau_k, t)$, the MIMO channel with N_t transmit antennas and N_r receiver antennas is given by the $N_r \times N_t$ matrix $h(\tau_k, t)$ as

$$H(\tau_k, t) = \begin{bmatrix} h_{1,1}(\tau_k, t) & h_{1,2}(\tau_k, t) & \dots & h_{1,N_t}(\tau_k, t) \\ h_{2,1}(\tau_k, t) & h_{2,2}(\tau_k, t) & \dots & h_{2,N_t}(\tau_k, t) \\ \vdots & \vdots & \ddots & \vdots \\ h_{N_r,1}(\tau_k, t) & h_{N_r,2}(\tau_k, t) & \dots & h_{N_r,N_t}(\tau_k, t) \end{bmatrix} \quad (A\text{-}1)$$

Further, given that the signal $s_j(t)$ is launched from the jth transmit antenna, the signal, $y_j(t)$, received at the ith receive antenna, is given by

$$y_i(t) = \sum_{j=1}^{N_t} \sum_{k=0}^{L-1} h_{i,j}(\tau_k, t) s_j(t - \tau_k) \quad (A\text{-}2)$$

For the ideal MIMO channel, each $h_{i,j}$ (drop the τ_k, t for convenience) has the same property as a SISO wireless channel where all the channels are independent and uncorrelated. In a realistic MIMO channel, there exists some degree of correlation between the channels and as a result, directly affects the diversity gains achievable by the MIMO system.

Defining the ideal channel matrix as H_w and the realistic channel matrix as H, it is known that H can deviate significantly from H_w as the result of the spatial correlation characteristics previously discussed. Correlation in the MIMO channel implies that the elements of H are correlated and may be modeled by

$$\text{vec}(H) = R^{1/2} \text{vec}(H_w) \quad (A\text{-}3)$$

Where R is the correlation matrix previously defined in the section titled *Combined spatial and antenna polarization correlation*. If $R = I_{N_t N_r}$, then $H = H_w$. Although the model described above is capable of capturing any correlation effects between the elements of H, a simpler and less generalized model is often adequate and is given by

$$H = R_r^{1/2} H_w R_t^{1/2} \qquad (A\text{-}4)$$

Where R_r and R_t are positive definite Hermitian matrices that specify the receive and transmit correlations, respectively. Note that when describing the BS as the transmitter and the MS as the receiver, $R_t = R_{BS}$ and $R_r = R_{MS}$, respectively. It can be shown that R, R_t, and R_r are related by

$$R = R_t \otimes R_r \qquad (A\text{-}5)$$

Where $\otimes$ denotes Kronecker product.

Channel capacity is defined as the maximum error-free data rate that a channel can support. In an independent, identically distributed (i.i.d.) Rayleigh fading environment, the capacity of a MIMO system with N_t transmit antennas and N_r receive antennas is defined as

$$C = \log_2 \det\left(I_{N_r} + \frac{\psi}{N_t} H_w H_w^H\right) = \sum_{i=1}^{N_r} \log_2\left(1 + \frac{\psi}{N_t}\mu_i\right) \qquad (A\text{-}6)$$

Where μ_i denotes the eigenvalues of $H_w H_w^H$, ψ may be interpreted as the average SNR at each of the receive antennas. The channel capacity scales almost linearly with $\min(N_t, N_r)$ for high SNR. This linear growth is due to the fact that in a richly scattered MIMO channel, path gains between different transmit/receive antenna pairs tend to fade independently, which makes it likely that multiple parallel channels will be formed, allowing several independent data streams to be transmitted simultaneously. In a practical MIMO channel, the capacity potential offered by multiple antennas suffers from correlation between local antenna elements. With the correlated channel model described in Equation (A-4) above, the capacity of the MIMO channel in the presence of fading correlation is

$$C = \log_2 \det\left(I_{N_r} + \frac{\psi}{N_t} R_r^{1/2} H_w R_t H_w^H R_r^{H/2}\right) \qquad (A\text{-}7)$$

This capacity equation assumes that the transmitter does not have any knowledge of the channel characteristics.

Assuming that the number of transmit and receive antennas are the same, $N_r = N_t = N$, and the transmit and receive correlation matrices, R_t and R_r, are full rank, implying that the elements of the matrices are not correlated, then at high SNR, the capacity of the MIMO channel can be written as

$$C \approx \log_2 \det\left(\frac{\psi}{N} H_w H_w^H\right) + \log_2 \det\left(R_r\right) + \log_2 \det\left(R_t\right) \quad \textit{(A-8)}$$

From this equation it is clear that R_r and R_t have the same impact on the capacity of the MIMO channel and the loss in capacity is given by

$$\log_2 \det\left(R_r\right) + \log_2 \det\left(R_t\right) \quad \textit{(A-9)}$$

Since the channel state, H, is random, the capacity associated with the MIMO channel is a random variable. The ergodic capacity, $\overline{C}$, of a MIMO channel is the ensemble average of the information rate over the distribution of the elements of the channel matrix, H.

$$\overline{C} = E\left\{\log_2 \det\left(I_{Nr} + \frac{\psi}{N_t} R_r^{1/2} H_w R_t H_w^H R_r^{H/2}\right)\right\} \quad \textit{(A-10)}$$

Appendix B: SNR for Uncorrelated and Correlated MIMO Channels

It can be shown that when MIMO channels are uncorrelated, and therefore defined as independent and identically-distributed (i.i.d), the following assumption can be satisfied

$$E\left[\sum_{j=1}^{M_t}|h_{ij}|^2\right] = E\left[\sum_{j=1}^{M_t}|h_{kj}|^2\right] \text{ with } 1 \le i \text{ and } k \le M_r \qquad (B\text{-}1)$$

as long as

$$E[|x_i|^2] = E[|x_j|^2] = \sigma^2 \text{ with } 1 \le i \text{ and } j \le M_t \qquad (B\text{-}2)$$

Then the power of received signal at any antenna is

$$E[|y_i|^2] = E[|y_j|^2] = E\left[\sum_{j=1}^{M_t}|h_{ij}|^2\right] * E[|x_k|^2] \qquad (B\text{-}3)$$

$$\text{with } 1 \le i \text{ and } j \le M_r \text{ and } 1 \le k \le M_t$$

This shows that the power of the received signal at each antenna is identical, and equal to the sum of the power from different transmitting antennas. Thus, we can use the SNR at each receiver to define the system SNR as was the case for the SISO system. If the channel matrix is normalized such that,

$$E\left[\sum_{j=1}^{M_t}|h_{ij}|^2\right] = E\left[\sum_{=1}^{M_t}|h_{kj}|^2\right] = M_t \text{ where } 1 \le i \text{ and } k \le M_r \qquad (B\text{-}4)$$

then the total transmitted signal power is P_T and the signal power at each transmit antenna is P_T/M_T. The received signal at each antenna is then P_T. The covariance of the elements of N is thus P_T/SNR. In this case, the measured signal power at the transmitter or the receiver can be used to calculate the noise power required to achieve a specified SNR.

In a practical situation, there is usually some level of spatial correlation in the MIMO channel. The spatial correlation is usually introduced into the ideal channel matrix, H_w, whose elements follow

$$\text{vec}(H) = R^{1/2}\text{vec}(H_w) \qquad (B\text{-}5)$$

The main difficulty in replacing H in

$$Y = HX + N \qquad \textit{(B-6)}$$

with the correlated H_r, using Equation (B-5), is that Equation (B-3) may no longer be valid as the power at any one receive antenna may be different from the others. In this case, the receiver power may not be used to define SNR. However, as discussed for the uncorrelated case above, it is also possible to define the SNR according to the transmitted signal power.

For the spatial correlation matrix, R, the diagonal elements are 1 and can be represented as

$$R = R^{1/2} * (R^{1/2})^{H} \qquad \textit{(B-7)}$$

where $R^{½}$ is defined as a Cholesky decomposition. Let $C = R^{½}$. Then, it can be shown that

$$E[\sum_{j=1}^{M_t M_r} |c_{ij}|^2] = R_{ii} = R_{kk} = E[\sum_{j=1}^{M_t M_r} |c_{kj}|^2] = 1 \qquad \textit{(B-8)}$$

$$\text{where } 1 \le i \text{ and } k \le M_t M_r$$

Since h_{ij} is uncorrelated and i.i.d, it can be further shown that

$$E[|h_{r,ij}|^2] = E[\sum_{j=1}^{M_t M_r} |c_{ij} Vec\,(H)_j|^2] = E[\sum_{j=1}^{M_t M_r} |c_{ij}|^2 |Vec\,(H)_j|^2] \qquad \textit{(B-9)}$$

$$= \sum_{j=1}^{M_t M_r} E[|c_{ij}|^2 |Vec\,(H)_j|^2] = E[|Vec\,(H)_k|^2] \sum_{j=1}^{M_t M_r} E[|c_{ij}|^2]$$

$$= E[|Vec\,(H)_k|^2] = G^2$$

$$\text{with } 1 \le k \le M_t M_r \text{ and } 1 \le i \le M_r \text{ and } 1 \le j \le M_t$$

If the H_r is normalized such that,

$$E[\sum_{i=1}^{M_t} |h_{r,ij}|^2] = E[\sum_{i=1}^{M_t} |h_{r,kj}|^2] = M_t \text{ with } 1 \le i,\ k \le M_r$$

then the normalization value should be $\sqrt{E[|h_{r,ij}|^2]} = G$. Defining the SNR at the transmitter, the covariance of the elements of N should be GP_T/SNR. Thus, to apply the SNR at the transmitter, the signal power is calibrated at the source and the channel gain is tracked according to the channel model. Based on these values, the covariance of the elements of N can be determined in order to achieve a required SNR.

Agilent Email Updates

www.agilent.com/find/emailupdates
Get the latest information on the products and applications you select.

Agilent Channel Partners

www.agilent.com/find/channelpartners
Get the best of both worlds: Agilent's measurement expertise and product breadth, combined with channel partner convenience.

Remove all doubt

Our repair and calibration services will get your equipment back to you, performing like new, when promised. You will get full value out of your Agilent equipment throughout its lifetime. Your equipment will be serviced by Agilent-trained technicians using the latest factory calibration procedures, automated repair diagnostics and genuine parts. You will always have the utmost confidence in your measurements.

Agilent offers a wide range of additional expert test and measurement services for your equipment, including initial start-up assistance onsite education and training, as well as design, system integration, and project management.

For more information on repair and calibration services, go to

www.agilent.com/find/removealldoubt

www.agilent.com
www.agilent.com/find/PXB

For more information on Agilent Technologies' products, applications or services, please contact your local Agilent office. The complete list is available at:

www.agilent.com/find/contactus

Americas

Canada	(877) 894-4414
Latin America	305 269 7500
United States	(800) 829-4444

Asia Pacific

Australia	1 800 629 485
China	800 810 0189
Hong Kong	800 938 693
India	1 800 112 929
Japan	0120 (421) 345
Korea	080 769 0800
Malaysia	1 800 888 848
Singapore	1 800 375 8100
Taiwan	0800 047 866
Thailand	1 800 226 008

Europe & Middle East

Austria	43 (0) 1 360 277 1571
Belgium	32 (0) 2 404 93 40
Denmark	45 70 13 15 15
Finland	358 (0) 10 855 2100
France	0825 010 700*
	*0.125 €/minute
Germany	49 (0) 7031 464 6333
Ireland	1890 924 204
Israel	972-3-9288-504/544
Italy	39 02 92 60 8484
Netherlands	31 (0) 20 547 2111
Spain	34 (91) 631 3300
Sweden	0200-88 22 55
Switzerland	0800 80 53 53
United Kingdom	44 (0) 118 9276201

Other European Countries:
www.agilent.com/find/contactus

Revised: October 1, 2009

Product specifications and descriptions in this document subject to change without notice.

Printed in USA, January 22, 2010
5989-8973EN

Agilent Technologies